Cellular and Molecular Life Sciences

https://doi.org/10.1007/s00018-025-05981-6

Article in Press

Oxysterol-mediated modulation of intestinal inflammation: insights into sex differences and GPR183 signaling

Received: 26 June 2025

Accepted: 2 November 2025

Published online: 15 December 2025

Cite this article as: Ameraoui H., Bestard-Escalas J., Roumain M. *et al.* Oxysterol-mediated modulation of intestinal inflammation: insights into sex differences and GPR183 signaling. *Cell. Mol. Life Sci.* (2025). https://doi.org/10.1007/s00018-025-05981-6

Hafsa Ameraoui, Joan Bestard-Escalas, Martin Roumain, Adam Laghouati, Pauline Bottemanne, Mireille Alhouayek & Giulio G. Muccioli

We are providing an unedited version of this manuscript to give early access to its findings. Before final publication, the manuscript will undergo further editing. Please note there may be errors present which affect the content, and all legal disclaimers apply.

If this paper is publishing under a Transparent Peer Review model then Peer Review reports will publish with the final article.

ARTICLE IN PRESS

© The Author(s) 2025. **Open Access** This article is licensed under a Creative Commons Attribution-NonCommercial-NoDerivatives 4.0 International License, which permits any non-commercial use, sharing, distribution and reproduction in any medium or format, as long as you give appropriate credit to the original author(s) and the source, provide a link to the Creative Commons licence, and indicate if you modified the licensed material. You do not have permission under this licence to share adapted material derived from this article or parts of it. The images or other third party material in this article are included in the article's Creative Commons licence, unless indicated otherwise in a credit line to the material. If material is not included in the article's Creative Commons licence and your intended use is not permitted by statutory regulation or exceeds the permitted use, you will need to obtain permission directly from the copyright holder. To view a copy of this licence, visit http://creativecommons.org/licenses/by-nc-nd/4.0/.

ARTICLE IN PRESS

Oxysterol-Mediated Modulation of Intestinal Inflammation: Insights into Sex Differences and GPR183 Signaling.

Hafsa Ameraoui[1], Juan Bestard-Escalas[1], Martin Roumain[1], Adam Laghouati[1], Pauline Bottemanne[1], Mireille Alhouayek[1], Giulio G Muccioli[1,*]

[1]Bioanalysis and Pharmacology of Bioactive Lipids Research Group, Louvain Drug Research Institute, Université catholique de Louvain, UCLouvain, Belgium

*** Corresponding author:**

Giulio G. Muccioli

Bioanalysis and Pharmacology of Bioactive Lipids Research Group, Louvain Drug Research Institute, Université catholique de Louvain, Av. E. Mounier, 72 (B1.72.01), 1200 Brussels, Belgium

Tel: +32 2 764 7231, giulio.muccioli@uclouvain.be

ARTICLE IN PRESS

Acknowledgments

This work was supported by subsidies from the 'Fonds Spéciaux de Recherches' [FSR, UCLouvain] and from the Fonds de la Recherche Scientifique [FRS-FNRS]. HA was a research fellow from the FRS-FNRS and was also supported by an ARC grant (UCLouvain). JBE and PB are postdoctoral fellows from the FRS-FNRS. MA is a research associate of the FRS-FNRS.

The MASSMET platform [UCL, Belgium] is acknowledged for access to HPLC-MS. The Cytoflux platform is acknowledged for access to flow cytometers. Rose-Marie Goebbels is acknowledged for her skillful help with tissue section preparation.

ARTICLE IN PRESS

ARTICLE IN PRESS

Abstract:

Background and Aims: Oxysterols, oxidized derivatives of cholesterol, play complex roles in inflammatory processes, but their specific functions in inflammatory bowel diseases remain incompletely understood. This study investigates the roles of key oxysterols — 7α,25-dihydroxycholesterol, 25-hydroxycholesterol, 25-hydroxycholesterol-3-sulfate, and 4β-hydroxycholesterol — and potential sex differences in intestinal inflammation.

Methods: We used complementary approaches including dextran sulfate sodium-induced colitis, and ex vivo studies with colon explants, organoids, and immune cells to examine oxysterol properties. Principal component analysis was employed to analyze variance between disease and sex. In vivo administration of 7α,25-dihydroxycholesterol and NIBR189, an antagonist of its receptor GPR183, was performed to assess effects on inflammatory markers and immune cell trafficking.

Results: We observed sex-specific differences in both basal and colitis-induced oxysterol profiles, with female mice showing greater resistance to dextran sulfate sodium-induced inflammation and distinct patterns of oxysterol metabolism. Principal component analysis highlighted a separation of samples by both treatment and sex, with dextran sulfate sodium treatment accounting for approximately 55% of variance and sex differences explaining 25%. In vitro, 25-hydroxycholesterol-3-sulfate and 7α,25-dihydroxycholesterol decreased inflammatory cytokine expression in colon explants from female mice and reduced cytokine production in THP-1-derived macrophages in a dose-dependent manner. GPR183 antagonists decreased cell activation, suggesting constitutive receptor activity. In vivo 7α,25-dihydroxycholesterol administration showed modest effects on inflammatory markers but significantly decreased immune cell counts in lymph nodes, consistent with altered immune cell trafficking.

ARTICLE IN PRESS

ARTICLE IN PRESS

Conclusion: Our findings reveal sex-specific regulation of inflammatory processes by oxysterols and highlight the therapeutic potential of targeting these pathways in inflammatory bowel diseases.

Key words : IBD, 27-hydroxycholesterol, Inflammatory bowel diseases, CYP7B1, Cholesterol-25-hydroxylase; PBMC

ARTICLE IN PRESS

ARTICLE IN PRESS

1. Introduction

Inflammatory bowel diseases (IBD), including Crohn's disease (CD) and ulcerative colitis (UC), involve chronic relapsing inflammation of the digestive tract. Despite overlapping clinical features, CD and UC affect different parts of the digestive tract and exhibit distinct inflammatory profiles. Current management strategies aim to alleviate symptoms and maintain remission, but they are not curative, and some patients experience debilitating adverse events[1]. Thus, understanding the immune mechanisms underlying IBD pathogenesis remains an area of active research.

Oxysterols are lipid mediators derived from the oxidation of cholesterol. Among their properties, oxysterols have been shown to play significant roles in immune and inflammatory processes through multiple mechanisms[2]. They can both promote and suppress inflammation, depending on the molecular species, cellular context, and disease state[2, 3]. For instance, oxysterols like 25-hydroxycholesterol (25HC) can inhibit inflammatory responses by activating liver X receptors (LXR) in macrophages and suppressing NF-κB signaling pathways[4, 5]. Moreover, its sulfated derivative, 25-hydroxycholesterol-3-sulfate (25HC3S), shows promising anti-inflammatory properties that warrant further investigation[6, 7].

The di-hydroxylated oxysterol 7α,25-dihydroxycholesterol (7α25HC) plays a unique role in immune regulation, directing immune cell trafficking and positioning within lymphoid tissues through GPR183 signaling. This characteristic makes it of particular interest in inflammatory contexts[8-11]. Several oxysterols, such as 7β,27-dihydroxycholesterol and 7α,27-dihydroxycholesterol, act as natural ligands for retinoic acid receptor-related orphan receptor gamma t (RORγt), an important transcription factor driving Th17 cell differentiation, thereby promoting inflammatory T cell responses[12]. In contrast, 4β-hydroxycholesterol (4βHC), one of the most abundant circulating oxysterols in mice, remains poorly characterized in

ARTICLE IN PRESS

IBD, representing a significant knowledge gap in our understanding of oxysterol-mediated inflammatory mechanisms[13, 14].

Their context-dependent immunomodulatory capacity makes oxysterols important mediators in various inflammatory conditions, including IBD, atherosclerosis, and neurodegenerative disorders[3, 13, 15]. For instance, in atherosclerosis, oxysterols accumulate in arterial plaques where they modulate foam cell formation and inflammatory responses of vascular cells, with 27-hydroxycholesterol (27HC) promoting plaque progression by increasing inflammatory cytokine expression and TLR4/NF-κB signaling pathways in macrophages[16]. Conversely, activation of LXR and Peroxisome Proliferator-activated Receptor gamma (PPARγ) by 25HC3S in macrophages promotes downregulation of cholesterol synthesis and suppresses inflammatory responses[17-19].

In IBD, studies have shown that oxysterols and their synthetic enzymes are dysregulated in both patients and experimental models[13]. Patients with CD display altered levels of oxysterols, including 25HC, 4βHC and 7α25HC, in intestinal tissues[13, 20]. Furthermore, the expression of synthetic enzymes such as CYP7B1 and cholesterol-25-hydroxylase (CH25H) was correlated with disease severity[13, 20]. On the other hand, the genetic deletion of CH25H exacerbates experimental colitis in mice, while administration of 25HC improved intestinal barrier function and reduced inflammation[13, 15, 21].

Despite these observations, significant gaps remain in our understanding of the two-way interaction between oxysterols and intestinal inflammation. Therefore, we aimed to investigate the roles of four key oxysterols: 25HC, 25HC3S, 7α25HC, and 4βHC. To address these research questions, we employed a multi-model approach including colon explants, colon organoids, human cell lines, and experimental colitis models. Murine colon explants provide in vitro cultures of colon tissue

ARTICLE IN PRESS

samples, allowing us to study inflammatory responses while minimizing animal use[22]. Murine colon organoids are three-dimensional structures derived from mouse colon epithelial cells, cultured in vitro, and capable of self-renewal and differentiation. These organoids have become an essential tool for studying the development, maintenance, and regeneration of the colon epithelium[23]. By integrating these diverse experimental models, we sought to improve the understanding on how these oxysterols modulate intestinal inflammation.

2. Materials and methods

Chemicals and reagents. Hexadecyl-trimethylammonium bromide (HTAB), ethylenediaminetetraacetic acid (EDTA), o-dianisidine, oxysterols of interest, NIBR189, GSK682753A, T0070907, N-acetylcysteine, phorbol 12-myristate 13-acetate (PMA), lipopolysaccharides (LPS; E. coli O55:B5), gentamicin and Phytohemagglutinin (PHA) were purchased from Sigma-Aldrich (Bornem, Belgium). Lipid standards used for quantification were purchased from Avanti Polar lipids. Dextran sulfate sodium (DSS, average MW 40 kDa) was purchased from TdB Consultancy (Uppsala, Sweden). HPLC-grade chloroform, dichloromethane, isopropanol, hexane, and methanol, as well as MS-grade methanol and acetonitrile, were purchased from VWR. B27, N2 supplement, collagenase type I, penicillin/streptomycin and all culture media (including RPMI 1640 medium with GlutaMAX™ Supplement, DMEM/F12, and DMEM high glucose with GlutaMAX™ Supplement) and the ELISA kits (Ready-Set-Go! Kit) were purchased from Life Technologies. Fetal bovine serum (FBS) was purchased from Gentaur. Primocin was from InvivoGen. Interferon gamma (IFNγ), tumor necrosis factor α (TNF-α), and epidermal growth factor (EGF) were obtained from Peprotech. Basement membrane extract-reduced growth factor (BME-RGF) matrix was obtained from R&D Systems. TriPure reagent was from Roche. The RT GoScript mix (Reverse

ARTICLE IN PRESS

Transcription System) and the qPCR GoTaq mix (GoTaq qPCR Master Mix with SYBR Green) were purchased from Promega. Primers were obtained from Integrated DNA Technologies. The DC protein assay kit was from Bio-Rad.

Mice. Male and female C57BL/6J mice, aged 8 weeks, were obtained from Janvier labs and allowed to acclimatize for one week in controlled conditions of temperature (20-22°C) and a 12h light-dark cycle. Mice were housed in standard filter-top cages with food and drinking water provided ad libitum. All animal experiments were conducted in accordance with the European directive 2010/63/EU and the Belgian Law of May 29, 2013 regarding the protection of laboratory animals, and approved by the local ethics committee of the UCLouvain (study agreements 2017/UCL/MD/024, 2021/UCL/MD/066 and 07-OTLADDB-2023-7, laboratory agreement LA1230635).

Induction of acute DSS colitis in mice. As we previously reported, to induce acute colitis, mice (N=8) were given 5% DSS in their drinking water for 5 days, followed by an additional 2 days of normal drinking water[13, 24, 25]. Control mice were given only normal drinking water throughout the study. Body weight was monitored daily. To evaluate the effects of 7α25HC and the GPR183 antagonist NIBR189, we employed an experimental design with the following treatment groups: 7α25HC (10 mg/kg), NIBR189 (10 mg/kg), a combination of 7α25HC and NIBR189 (10 mg/kg each), and a vehicle control[10, 26]. Compounds were administered intraperitoneally (i.p.) once daily in a vehicle solution composed of saline-DMSO-Tween 80 (18:1:1, v/v/v). Treatment was started on the first day of DSS administration in the drinking water.

On day 7, mice were anesthetized using isoflurane and blood was collected prior to euthanasia. Following euthanasia, colons were precisely dissected, cleaned and measured for weight and length to assess macroscopic damage[25]. Spleens and livers were also collected and weighed. All tissues were snap frozen in liquid

ARTICLE IN PRESS

nitrogen and stored at -80°C for later analysis using real-time quantitative PCR (qPCR), myeloperoxidase activity assay, and lipid quantification by LC-MS. For histological assessment, tissues were fixed in 4% formaldehyde solution.

Histology. Colon slices fixed in formaldehyde were embedded in paraffin and sectioned into 5 µm-thick slices, which were then stained with hematoxylin and eosin. For each colon, two slides were prepared, each containing three serial sections (5 µm) with a 100 µm distance between the first and second sets of slices. In total, six sections per mouse were evaluated. The sections were scored in a blind fashion as we previously reported[13, 25]. Briefly, the microscopic scoring system used for the acute colitis model combined the infiltration score (0-4) and tissue damage score (0-3). The infiltration score ranged from 0 (no infiltration) to 4 (extensive infiltration of the muscularis propria), while the tissue damage score ranged from 0 (no structural damage) to 3 (extensive mucosal damage extending into deeper structures of the muscularis propria).

Murine colon explants preparation. DSS-treated C57BL/6J mice were euthanized according to institutional guidelines and approved protocols. The entire colon was carefully removed, and fecal content was gently flushed out using ice-cold phosphate-buffered saline (PBS). The colon was placed on a clean, sterile surface and longitudinally opened with fine scissors. Visible fat and connective tissues were removed, and the colon was then sectioned into 400 µm thick slices. The colon slices were transferred to a 24-well tissue culture plate (10-12 slices/well) containing 1 mL of RPMI 1640 medium with GlutaMAX™, supplemented with 10% fetal bovine serum (FBS), 100 U/mL penicillin, 100 µg/mL streptomycin, and 50 µg/mL gentamicin. The colon slices were incubated with oxysterols (1 µM and 10 µM) or vehicle (DMSO, 0.1%) for 8h at 37°C in a humidified atmosphere containing 5% CO_2. Following the incubation period, culture supernatants and

ARTICLE IN PRESS

ARTICLE IN PRESS

colon slices were collected and stored at -80°C for subsequent cytokine measurement and gene expression assessment.

Colon organoids. Colon crypts were isolated from male C57BL/6J mice according to the protocol published by Pleguezuelos-Manzano and colleagues[23]. Briefly, the colons were opened and washed for any feces residues. Then, the tissue was cut into small pieces and incubated for 30 minutes in PBS with 100 µg/ml of Primocin. After removing the PBS, the colon pieces were digested for 30 minutes with DMEM/F12 with 100 µg/ml Primocin and 500 U/ml of Collagenase type I for 30 minutes at 37 °C with vigorous shaking every 5 minutes. After the digestion, the digestion buffer was neutralized with 4 volumes of DMEM/F12 with 1% Primocin and 10% FBS and the medium was passed through a 100 µm mesh to collect colon crypts. The crypt suspension was pelleted (300 x g, 5min) and plated on a petri dish to separate the crypts from the adherent fibroblasts and macrophages. After 30 min, the crypts were pelleted (80 x g, 3 min) twice before being resuspended in cold Basement membrane extract-reduced growth factor matrix (BME-RGF) and plated in domes. To maintain the organoids, we used medium composed of 45% Wnt3a-RSPONDIN1-Noggin complemented medium 45% DMEM/F12, 10% FBS, 100 µg/ml Primocin, 0.02% B27, 0.01% N2, 1 mM *N*-acetylcysteine, 50 ng/ml EGF and 0.1% HEPES. Wnt3a-RSPONDIN1-Noggin complemented medium was obtained from L-WRN cells (Caltag Medsystems) maintained in culture following the supplier instructions.

For organoid passaging, we harvested the cultures by dissolving the BME domes in cold cell recovery solution, followed by gentle mechanical dissociation. The resulting organoid fragments were collected by centrifugation and reseeded in fresh BME-RGF at 25% of the initial density.

Inflammatory stimulation was achieved by treating the organoids with a combination of LPS (1 µg/mL) and IFNγ (10 ng/mL), with concurrent treatment with

ARTICLE IN PRESS

oxysterols (1 or 10 µM). Control organoids were maintained in parallel and received equivalent volumes of vehicle (0.1% DMSO). The cultures were incubated for 8h at 37°C in a humidified atmosphere containing 5% CO_2. Following the incubation period, both culture media and organoid samples were collected and stored at -80°C for subsequent analyses.

THP-1 culture and differentiation. The human monocytic cell line THP-1 (European Collection of Authenticated Cell Cultures, 88081201) was maintained in DMEM medium with high glucose and GlutaMAX™, supplemented with 10% FBS, 100 U/mL penicillin, and 100 µg/mL streptomycin. Cells were cultured at 37°C in a humidified atmosphere containing 5% CO_2.

For differentiation into macrophages, THP-1 monocytes were seeded at a density of 10^5 cells/mL in 24-well plates. Cells were treated with PMA (50 nM) for 48h. After incubation, the medium was replaced with fresh RPMI 1640 medium containing 10% FBS, 100 U/mL penicillin, and 100 µg/mL streptomycin, and cells were allowed to rest for an additional 24h to ensure full differentiation.

To activate the cells, THP-1-derived macrophages were incubated with LPS (100 ng/mL) and IFNγ (10 ng/mL). To assess the effect of oxysterols, the cells were co-incubated with oxysterols (1 µM or 10 µM) or vehicle (DMSO, 0.1%) for 8h. After the incubation period, culture supernatants and cells were collected and stored at -80°C for subsequent cytokine measurement and gene expression assessment.

Caco-2 culture and treatment. The human colon adenocarcinoma Caco-2 cell line was purchased from the American Type Culture Collection (cat#: HTB-37). The cells were cultured in DMEM medium with high glucose and GlutaMAX™, supplemented with 10% FBS, 100 U/mL penicillin, and 100 µg/mL streptomycin. The cells were seeded at a concentration of 5×10^5 onto 12-well Thincerts with a 0.4 µm pore diameter (Greiner, cat# 665640), with 500 µL of medium in the apical

ARTICLE IN PRESS

compartment and 1.5 mL in the basolateral compartment. The media were renewed every 2 days, and the cells were cultured for 21 days.

The transepithelial electrical resistance (TEER) was measured using an EndOhm chamber connected to a EVOM2 resistance meter (World Precision Instruments) to assess the barrier development of the Caco-2 cell layer. TEER was assessed after 16, 18, 20, and 21 days in culture, as previously described by Kämpfer and colleagues[27].

On day 20, LPS (1000 ng/mL), TNF-α (25 ng/mL), and IFNγ (10 ng/mL) were added to the basolateral compartment together with the oxysterols (1 µM or 10 µM) or vehicle (DMSO, 0.1%). The cells were incubated for 24h at 37°C in a humidified atmosphere containing 5% CO_2. Following the incubation period, both cells and culture media were collected and stored at -80°C for subsequent analysis.

PBMC Isolation and treatment. Peripheral blood samples were obtained from healthy donors following informed consent. This study was approved by the ethics committee of UCLouvain and its affiliated hospital (cliniques universitaires Saint Luc) (2023/06JUI/252 - Belgian registration number: B4032023000052). Blood was collected into vacutainer tubes containing EDTA as an anticoagulant. Peripheral blood mononuclear cells (PBMC) were isolated using density gradient centrifugation with Ficoll-Paque PLUS (GE Healthcare) according to the manufacturer's instructions. Briefly, the blood was diluted 1:1 with PBS and layered onto Ficoll-Paque PLUS in a 50 mL Leucosep centrifuge tube. Centrifugation was performed at 800×*g* for 30 minutes at room temperature with no brake. The PBMC layer was collected, transferred to a new 50 mL centrifuge tube, and after an ACK incubation step, washed twice with sterile PBS. The final cell pellet was resuspended in RPMI 1640 medium with GlutaMAX™, supplemented with 10% FBS, 100 units/mL penicillin, and 100 µg/mL streptomycin.

ARTICLE IN PRESS

PBMC were seeded at a density of 10^6 cells/mL in 24-well plates in a total volume of 1 mL/well and treated 16h later. For LPS stimulation, the cells were treated with 1 µg/mL LPS and co-treated oxysterols (1 or 10 µM). Control conditions were obtained by incubating the cells with vehicle (DMSO 0.1%). Cells were incubated at 37°C in a humidified atmosphere containing 5% CO_2 for 8h.

For phytohemagglutinin (PHA) stimulation, the cells were treated with 5 µg/mL PHA and incubated at 37°C in a humidified atmosphere containing 5% CO_2. After 24h, oxysterols (1 µM or 10 µM) or vehicle (DMSO 0.1%) were added to the cells for 24 additional hours.

For both stimulation protocols, at the end of the incubation period the cells and the supernatants were separately collected and stored at -80°C for subsequent analysis.

Gene expression by real-time quantitative polymerase chain reaction (qPCR). Total RNA from colon tissues and cells was extracted using TriPure reagent according to the manufacturer's protocol as previously described[25]. In colon tissue from DSS experiments, we used lithium chloride purification to eliminate DSS contamination that may inhibit the reverse transcription reaction, as previously reported[24, 28]. Complementary DNA (cDNA) was synthesized from purified total RNA (1.6 µg) using a reverse transcription kit (GoScript Reverse Transcription System from Promega). The reaction comprised three steps: primer annealing at 25°C, cDNA polymerization at 42°C for 1 hour, and enzyme deactivation at 70°C for 15 minutes. qPCR was performed using the GoTaq qPCR Master Mix with SYBR Green from Promega, on a QuantStudio 3 Real-Time PCR System (Thermo Fisher Scientific).

Gene	**Product**	**Forward primers (5′-3′)**	**Reverse primer (3′-5′)**
Murine primers			
Gene		**Forward**	**Reverse**

ARTICLE IN PRESS

Ccl2	MCP-1	GTCCCAAAGAAGCTGTAGTTTTTG	ATGTATGTCTGGACCCATTCC
Ch25h	CH25H	CTGACCTTCTTCGACGTGCT	GGGAAGTCATAGCCCGAGTG
Cxcl1	KC	GGCTGGGATTCACCTCAAG	GAGTGTGGCTATGACTTCGG
Cxcl2	MIP2α	CAGACAGAAGTCATAGCCACTC	CCTTTCCAGGTCAGTTAGCC
Cyp3a11	CYP3A11	GAAGCATTGAGGAGGATCACA	GTGCCTAAAAATGGCAGAGG
Cyp3a13	CYP3A13	AATAAGGCACCTGCCACCTATG	ACAGACCCTCTCAAGTCTTCC
Cyp7b1	CYP7B1	TAGGCATGACGATCCTGAAA	TCTCTGGTGAAGTGGACTGAAA
Cyp27a1	CYP27A1	GGCTACCTGCACTTCCT	CTGGATCTCTGGGCTCTTTG
Ebp	CHEH	AGGGCTGGTTCTCTCTCTAC	CGACGAAGCTGTCACTAAGG
Esr1	ERα	CCGCCTTCTACAGGTCTAATTC	CGTTACTGCTGGACAGTCTC
Hsd3b7	HSD3B7	CAGTCCACAGCCATCCCTACC	CGTGGGTCGAAGGGCACA
Hsd11b1	HSD11B1	CCTTGGCTGGGAAAATGACCC	AGGACACAGAGAGTGATGGACA
Il1b	IL-1β	TGTCTTTCCCGTGGACCTTC	CCAGCAGGTTATCATCATCATCCC
Il6	IL-6	ACAAGTCGGAGGCTTAATTACACAT	TTGCCATTGCACAACTCTTTTC
Gpr183	GPR183	CTGCATGGACCCGTTCATATAC	GGAGATCGACACACTCACTTG
Nr1h3	LXRα	ACCAGCTCCAAGTAGAGAGG	GCATCCGTGGGAACATCAG
Nr1h2	LXRβ	TGAAGGCGTCCACCATTG	CGTCCTTGCTGTAGGTGAAG
Pparg	PPARγ	GCATTTCTGCTCCACACTATG	GATCGCACTTTGGTATTCTTGG
Rorc	RORγ	GGATGAGATTGCCCTCTACAC	CAGATGTTCCACTCTCCTCTTC
Rpl19	RPL19	GAAGGTCAAAGGGAATGTGTTCA	CCTTGTCTGCCTTCAGCTTGT
Sult2b1	SULT2B1	GCTCCAAGGCTAAGGTGATTT	TGAAGGAACTGGTCGGGTGT
Tnf	TNFα	CTACTGAACTTCGGGGTGATC	TGAGTGTGAGGGTCTGGGC
Human primers			
ESR1	ERα	CCCAGGGAAGCTACTGTTTG	GCGGAACCGAGATGATGTAG
IFNG	IFNγ	GTGTGGAGACCATCAAGGAA	GCGTTGGACATTCAAGTCAG
GPR183	GPR183	CACCCTCTACGCTACAACAAG	AGGAGTGGGAGTGTCTGAG
IL13	IL-13	TCGAGAAGACCCAGAGGATG	GAGCAGGTCCTTTACAAACTGG

ARTICLE IN PRESS

NR1H2	LXRβ	CATCCACTATCGAGATCATGCTG	CGTCCTTGCTGTAGGTGAAG
NR1H3	LXRα	TACGTCTCCATCCACCATCC	GGAGGCTCACCAGTTTCATTAG
PPARG	PPARγ	GGTGACTTTATGGAGCCCAAG	GCGGTCTCCACTGAGAATAATG
RORC	RORγ	CAATCTGGAGCTGGCCTTTC	TTGGGTGGCAGCTTTGC
RPL19	RPL19	CACATCCACAAGCTGAAGGCA	CTTGCGTGCTTCCTTGGTCT

Myeloperoxidase (MPO) Assay

As previously described, colon samples were homogenized in potassium phosphate buffer (KH_2PO_4, pH 6.0), containing 0.5% hexadecyltrimethylammonium bromide (HTAB) using a Tissue Lyser (30 Hz for 3 minutes) with stainless steel beads[24]. The homogenate was then centrifuged at 15,000 x *g* for 20 minutes at 4°C. A total of 7 µL of supernatant was added to 96-well plates together with 200 µL of a solution of 0.167 mg/mL o-dianisidine and 5 ppm hydrogen peroxide in potassium phosphate buffer (50 mM, pH 6). Samples were analyzed in duplicate. Total protein concentration was determined using DC protein assay (Bio-Rad) and used to normalize the data. MPO activity was measured spectrophotometrically at 460 nm and normalized for protein concentration.

Enzyme-linked immunosorbent assay (ELISA). Cytokine levels were measured using Ready-Set-Go! Kit according to the manufacturer's instructions. For determination of cytokine release in the culture media, 100 µL of culture media was used. For colon tissues, colon samples were homogenized in phosphate buffer (pH 7) containing 0.05% Triton X-100 and centrifuged at 15,000 x *g* for 15 minutes at 4°C. For colon samples, the total protein concentration was determined using the DC protein assay and used for cytokine level normalization.

Flow cytometry. Freshly isolated mesenteric lymph nodes were used for flow cytometric staining and analysis. Single-cell suspensions from mesenteric lymph nodes were prepared by mechanical dissociation, by triturating the nodes with the flat end of a syringe plunger in gentle circular motions. The cell suspension was

passed through 70-µm filters to remove undigested debris. The collected cells were fixed in 4% paraformaldehyde solution (PFA) for 15 minutes, washed with PBS/EDTA 0.5mM to remove PFA, and labeled with fluorophore-conjugated antibodies from Miltenyi® (10 min in the dark). Fluorophore-conjugated antibodies included CD19 PE (clone REA675), F4/80 FITC (clone REA126), CD11c APC (clone REA754), Ly6C PE-Vio 770 (clone REA796), CD11b APC-Vio 770 (clone REA592), CD4 Vioblue (clone REA604), CD8a PerCP-Vio 700 (clone REA601), CD45 VioGreen (clone REA747). The unbound antibodies were washed off by centrifugation after washing with PBS/EDTA 0.5mM and the cells were resuspended in PBS/EDTA 0.5mM. The different cell populations were acquired on BD FACS Canto II and analyzed using Forward Scatter (FSC) and Side Scatter (SSC) followed by doublets exclusion, on FlowJo® version X.

Oxysterol quantification. Oxysterol levels were determined using a validated LC-HRMS method as previously described[29, 30]. Briefly, homogenized colon tissues or plasma were placed in glass vials containing deuterated internal standards (133.3 pmol d7-4β-hydroxycholesterol, 200 pmol d7-24(*R/S*)-hydroxycholesterol), dichloromethane, methanol (containing 10 µg butylated hydroxytoluene) and water (containing 20 ng EDTA) (4:2:1, v/v/v). Samples were subsequently sonicated in an ice-cold water bath for 10 min prior to centrifugation (600 × g, 10 min, 4°C). Organic phases were recovered and dried under a nitrogen stream. Lipids were then resuspended in dichloromethane and transferred on unmodified silica column for purification by solid-phase extraction. Oxysterols were recovered using 3.5 mL *n*-hexane – isopropanol after eliminating cholesterol and other highly hydrophobic compounds using 6 mL *n*-hexane – isopropanol (99:1, v/v)[31]. Eluates were dried under a nitrogen stream and the residue was resuspended in 30 µL methanol and stored at -20°C before analysis.

The LC-HRMS system was composed of an Accela LC pump and autosampler coupled to an LTQ-Orbitrap XL high resolution mass spectrometer (Thermo Fisher Scientific) equipped with an APCI probe used in positive mode. Chromatographic separation was achieved using an AscentisExpress C18 column (150 × 4.6 mm; 2.7 µm, Sigma-Aldrich), kept at 15°C. The mobile phase consisted in a gradient of methanol and water containing acetic acid. Calibration curves underwent the whole analytical process.

Statistical analysis. GraphPad Prism 9.0 software was used for statistical analysis. Data distribution normality was assessed using the Shapiro-Wilk test. For normally distributed data, one-way ANOVA followed by Sidak's post-hoc test was employed for multiple group comparisons. In case of unequal variances, the Brown-Forsythe and Welch ANOVA tests were used followed by Dunnett T3 post hoc test. Two-way ANOVA with Sidak’s post-hoc test was used to evaluate the effects of sex, treatment and treatment concentration. For non-parametric data, Mann-Whitney test or Kruskal-Wallis test was applied. Statistical significance was established at $p < 0.05$.

PCA and correlation analyses were performed using R statistical software (R Core Team, 2024) in RStudio (version 2024.04.2+764) (https://cran.r-project.org/). For PCA, oxysterol data were scaled (centered and standardized) before analysis. Correlation coefficients (r) were calculated and visualized as heatmaps using the ggplot2 package, with statistical significance indicated ($P < 0.05$, $P < 0.01$, $P < 0.001$). Separate correlation matrices were generated for male and female mice to identify sex-specific patterns.

ARTICLE IN PRESS

3. Results

DSS-induced colitis differently alters the inflammatory tone and oxysterols levels in male and female mice.

To investigate the role of oxysterols in intestinal inflammation, we used the DSS-induced colitis mouse model, a well-established experimental system that recapitulates key features of IBD[32], including epithelial damage, inflammatory cell infiltration, and altered mucosal barrier function[33]. Given the emerging evidence of sex-specific differences in IBD pathogenesis and progression, we specifically designed our study to examine both male and female mice, addressing the critical gap in understanding sex-specific variations in oxysterol metabolism and inflammatory responses during colitis[34].

As expected, DSS administration induced a decrease in mice body weight (Supplementary Figure 1) and an increase in the colon weight over length ratio (Figure 1A). Similarly, MPO activity, which is linked to neutrophil presence in the tissue, was increased in the groups receiving DSS (Figure 1B). Male and female mice showed differential responsiveness to DSS-induced colitis, with females exhibiting greater resistance, as suggested by lower TNF-α and MCP-1 gene expression in colon tissue and reduced IL-6 protein levels in colon explant supernatants (Figure 1C, D). Regarding the oxysterols, we found differences in the levels of several oxysterols between male and female mice (Figure 1E). For instance, under control conditions, the levels of 7-ketocholesterol (7KC), 5α,6α-epoxycholesterol, and 5β,6β-epoxycholesterol were lower in the colons of female mice compared to male mice. The levels of 5α,6α-epoxycholesterol, and 5β,6β-epoxycholesterol remained unchanged in the DSS conditions, with lower levels in females compared to males, while 7KC was increased following colon inflammation in female mice (Figure 1E). Further differences were seen, in the DSS condition, in

ARTICLE IN PRESS

the levels of 7-hydroxycholesterol (7HC) and 7-keto-25-hydroxycholesterol (7K25HC) that were lower in the colons from female mice compared to male mice, while the levels of 24(*S*)-hydroxycholesterol and 27HC were higher in the colons of female mice. The principal component analysis (PCA) plot, obtained using oxysterol levels as variables, further highlights the differences in colon oxysterol profiles between the experimental groups (Figure 1F). The first principal component, PC1, accounts for 54.8% of the variance and separates the samples based on treatment. This indicates that the colon oxysterol composition is significantly different between the DSS-treated and control groups. The second principal component, PC2, explains 25% of the variance and appears to distinguish the samples by sex regardless of treatment. This suggests that there are inherent differences in colon oxysterol profiles between male and female animals. Of note we did not find differences in mRNA expression for the different receptors known to bind the oxysterols except for LXRα that was lower in females compared to males and LXRβ that was decreased upon colon inflammation in males (Supplementary Figure 2).

To explore the relationship between colitis and oxysterol levels, we examined the correlation between oxysterol levels and inflammatory markers measured in the colon (Figure 1G). In male mice, a significant correlation was observed between the levels of monohydroxylated oxysterols, including 4βHC, 7HC, 25HC, and 7K25HC and inflammatory markers such as TNF-α, MCP-1 and IL-6. However, in female mice, the correlation is limited to MPO activity and weight/length ratio, potentially due to the lower inflammatory tone in females.

Besides oxysterol levels, we also measured the mRNA expression of their metabolic enzymes. Expression of CYP7B1 and CH25H was increased by colitis while expression of HSD3B7 was decreased (Supplementary Figure 3A). These three enzymes play a crucial role in regulating 7α,25-dihydroxycholesterol (7α25HC) levels in lymph nodes[35]. Notably, we found a strong positive correlation between

ARTICLE IN PRESS

inflammatory markers and the expression of CYP7B1 and CH25H in the colon, alongside an inverse correlation with HSD3B7 in both male and female mice (Supplementary Figure 3B). Furthermore, SULT2B1, which is responsible for the sulfation of hydroxycholesterols such as 25HC, showed a negative correlation with inflammatory markers in males but not in females (Supplementary Figure 3B).

In the plasma, we also observe differences in oxysterol levels between male and female mice under control conditions (Figure 2A). For instance, the levels of 25HC, 7α-hydroxycholestenone (7αHCnone), and 7K25HC were higher in the plasma from female mice compared to males. With DSS-induced colitis, the levels of 7αHCnone and 22(*R*)HC were higher in female mice (Figure 2A). Interestingly, the plasma levels of 4βHC were increased by the colitis in both males and females while the levels of 7K25HC and 27HC were increased in male mice with DSS treatment but not significantly increased in females (Figure 2A).

The PCA revealed distinct differences in the plasma oxysterol profile between the experimental groups (Figure 2B). PC1 accounted for 59.7% of the total variance in the data, and separated the samples based on DSS treatment consistent with a shift in the overall plasma oxysterol composition in response to the colitis-inducing DSS challenge. Furthermore, the second principal component (PC2), explaining 19.8% of the variation, reflected sex-specific differences in oxysterol profiles. Moreover, female and male DSS groups exhibited larger dispersions compared to their CTL counterparts. (Figure 2B).

Taken together these findings indicate that there are sex-dependent differences not only in basal oxysterol levels, but also in the dynamic responses of specific oxysterol species to the colitis. The different patterns observed between the colon tissue and plasma suggest compartment-specific regulation of oxysterol metabolism in male versus female mice during colon inflammation.

ARTICLE IN PRESS

ARTICLE IN PRESS

Oxysterols decrease the inflammatory tone in isolated colon tissue.

Building on these data, we conducted a series of ex vivo experiments using colon explants from male and female mice as this model incorporates essential elements contributing to colon inflammation (including the presence of immune and epithelial cells). We focused on 25HC, 7α25HC, 25HC3S, and 4βHC due to their demonstrated interactions with critical inflammation-regulating receptors, and therefore, their relevance to inflammatory processes[36]. These receptors include LXRα and β, GPR183, estrogen receptor alpha (ERα), peroxisome proliferator-activated receptor gamma (PPARγ), and RORγ[2].

Thus, colon explants, prepared from male and female mice treated with DSS, were incubated with the oxysterols of interest. Our findings reveal that 25HC3S and, to a lesser extent, 7α25HC decrease the expression of MCP-1 and IL-6 in colon explants obtained from female mice but not in colon explants obtained from male mice (Figure 3). This observation provides valuable insights into the potential sex-specific effects of these oxysterols on inflammatory markers in the colon.

ARTICLE IN PRESS

While giving valuable information, explant-based experiments cannot discern between the effects on epithelial cells and on the immune cells. To study the epithelial component, we used colon organoids as this experimental setup represents a refined ex vivo reconstitution of the epithelium. Colon organoids were stimulated with LPS and IFNy and concurrently treated with oxysterols for 24h. Subsequently, we assessed the expression of inflammatory cytokines both within the organoids and in the culture media. As expected, the incubation with LPS and IFNγ resulted in an increased expression of several proinflammatory markers, namely KC, Mip2α and TNF-α (Figure 4). Although in these conditions the oxysterols had limited effects, we observed a downward trend in the expression of Mip2α (Figure 4A) and TNF-α levels (Figure 4B) following the treatment with 7α25HC at a

ARTICLE IN PRESS

concentration of 10 µM. Intriguingly, the opposite trend was noted with the lower concentration (i.e. 1 µM).

In addition to colon organoids, we used a complementary model involving epithelial components, namely Caco-2 cells. These cells were cultured on inserts and, upon differentiation, formed a monolayer mimicking the intestinal epithelium. To induce an inflammatory response, a combination of cytokines (TNF-α-IFNγ) and LPS was applied. Caco-2 monolayers were then co-treated with oxysterols for a duration of 24h. The activation resulted in elevated IL-8 production and a concurrent reduction in monolayer permeability, as evidenced by trans-epithelial electrical resistance (TEER) measurements (Supplementary figure 4). However, in these conditions, none of the oxysterols affected the TEER values or IL-8 levels (Supplementary figure 4).

Oxysterols decrease activation of THP-1 derived macrophages, but not human PBMC.

We then delved into investigating the impact of 25HC, 4βHC, 25HC3S and 7α25HC on immune cell activation using THP-1 derived macrophages and human PBMC.

First, THP-1 derived macrophages, obtained by incubating the human THP-1 cell line with PMA, were stimulated with LPS-IFNγ, and co-treated with oxysterols. Levels of IL-6 and TNF-α in the culture medium were increased by the pro-inflammatory stimulus and decreased by 4βHC, 25HC3S and 7α25HC (Figure 5A). In the same setting, we examined the expression of the most described oxysterol receptors. We noted that PMA-differentiated THP-1 cells exhibited differential expression of oxysterol receptors compared to undifferentiated THP-1 cells (Figure 5B). Overall, the expression of these receptors was upregulated with PMA and further induced upon LPS-IFNγ activation for LXRα and LXRβ, while it was restored to basal levels for PPARγ (Figure 5B). Subsequently, we aimed to explore whether

ARTICLE IN PRESS

the observed effects were mediated by GPR183 and PPARγ, the two most described receptors for 7α25HC and 25HC3S, respectively. In our conditions, co-incubation of 25HC3S with the PPARγ antagonist T0070907 did not reverse the effects of the oxysterol (Figure 5C). Similarly, NIBR189 and GSK682753A, two GPR183 antagonists, failed to reverse the effects of 7α25HC. In fact, GSK682753A per se had similar effects as the GPR183 endogenous ligand 7α25HC (Figure 5D). Although not clarifying the molecular target involved, these data support the anti-inflammatory properties of these oxysterols.

Next, we used PBMC isolated from volunteers' blood and assessed the effects of oxysterols in two different settings characterized by distinct types of activation. In the first setting, PBMC were activated with LPS and co-treated with oxysterols. Indeed, LPS levels are frequently increased in IBD due to the altered intestinal barrier. While LPS resulted in the expected increase of TNF-α and IL-6 levels in the medium, the four oxysterols tested had no effect (Figure 6A). As LPS activates only a subpopulation of PBMC (mainly monocytes[37]), in the second setting we treated the PBMC with PHA to activate the lymphocytes. PBMC treatment with PHA for 48h resulted in increased mRNA expression of IFNγ and IL-13, as well as increased TNF-α levels in the culture medium (Figure 6B, C). While 4βHC, and 25HCS3S had no effects in this setting, there was a decrease in IFNγ expression and TNF-α levels upon treatment with 25HC at 10μM and a decrease in TNF-α levels with 7α25HC at 10μM (Figure 6B, C). Of note, while LPS had a limited effect on the expression of the main oxysterol receptors besides a decrease in PPARy expression, PHA activation decreased the expression of LXRα, GPR183 and PPARy (Supplementary figure 5A, B). ERα expression could not be detected in PBMC.

ARTICLE IN PRESS

ARTICLE IN PRESS

Sex-specific immunomodulatory effects of 7α25HC and GPR183 antagonism in DSS-induced colitis

Colitis results in a strong activation of the 7α25HC pathway as illustrated by the increased mRNA expression of CH25H and CYP7B1. Moreover, this is correlated with disease extent in male but not in female mice. Given the limited data available on the effects of 7α25HC in colitis models, we investigated its effects in DSS-induced colitis both by intraperitoneally administering 7α25HC and by blocking its main receptor using the selective GPR183 antagonist, NIBR189[10, 26]. We conducted these experiments in both male and female mice to account for potential sex-specific differences in oxysterol metabolism and function[38, 39].

Both in male and female mice, DSS administration induced the classical signs of colitis including an increase in the colon weight over length ratio, an altered colon tissue histology and increased MPO activity (Figure 7 and Figure 8). The macroscopic and histological evaluation of colitis severity revealed no significant differences between the DSS mice treated with the vehicle and those treated with 7α25HC (10 mg/kg), NIBR189 (10 mg/kg), or their combination (10 mg/kg each) (Figure 7). Additionally, we assessed MPO activity and cytokine expression using qPCR and ELISA (Figure 8). The administration of 7α25HC had no effect on the measured markers besides a decrease in MPO activity and a trend to reduce IL-6 levels ($p = 0.08$) in male mice (Figure 8).

Furthermore, flow cytometry quantification of the immune cells in the mesenteric lymph nodes (Supplementary Figure 6) indicated decreased numbers of macrophages and dendritic cells in male mice treated with 7α25HC (Figure 9A). In female mice, 7α25HC administration decreased the numbers of monocytes and dendritic cells, as well as B cell, CD4 T cell, and CD8 T cell populations. In these mice, the administration of NIBR189 partially blocked the effect of the oxysterol on

ARTICLE IN PRESS

the CD4 T cell, and CD8 T cell populations but not those on myeloid mononuclear cells (Figure 9B).

4. Discussion

Previous studies have demonstrated sexual dimorphism in both murine models of colitis and human IBD, with significant differences in disease prevalence, progression, and treatment responses[34]. Our current study extends these findings by revealing sex-specific differences in both basal and colitis-induced oxysterol levels and metabolism. This observation adds to the growing body of evidence suggesting sex-specific regulation of sterol metabolism[40], which is particularly significant given the crucial role of oxysterols in inflammation and immune regulation[3, 41].

The present study provides several important insights into the anti-inflammatory effects and potential mechanisms of action of the oxysterols 7α25HC and 25HC3S. Notably, we observed sex-related differences in the anti-inflammatory effects of these lipid mediators, with more pronounced effects observed in female colon explants compared to their male counterparts. This aligns with previous reports of differences in oxysterol levels and their alterations in response to inflammatory stimuli between males and females[34, 42].

Our functional studies were focused on 7α25HC, 25HC, 25HC3S, and 4βHC due to our observations in DSS-induced colitis in males and females but also as a continuity to our previous works exploring these oxysterols in inflammatory models [7, 13]. Moreover, our finding of increased 27HC specifically in female mice with colitis provides an intriguing parallel pathway that may contribute to sex-specific disease patterns. As a dual SERM and LXR agonist, 27HC represents a promising candidate

ARTICLE IN PRESS

for future mechanistic and therapeutic investigations, particularly given the protective roles of both ERα and LXRβ in DSS-induced colitis[43 44, 45].

This sexual dimorphism aligns with previous findings demonstrating that estrogen regulates cholesterol homeostasis through multiple mechanisms, including the modulation of CYP7A1 expression and bile acid synthesis[38]. Furthermore, CYP7B1, another key enzyme in oxysterol metabolism, has been shown to be differentially regulated by sex hormones, potentially contributing to sex-specific oxysterol profiles[46]. This underscores the importance of considering sex as a biological variable when investigating the role of oxysterols in IBD.

To better understand the potential link between oxysterol metabolism and the divergent inflammatory responses observed between male and female mice in DSS colitis, we analyzed correlations between oxysterol-metabolizing enzymes and inflammatory markers. Interestingly, we observed, in the DSS-induced colitis mouse model, a coordinated regulation of enzymes involved in 7α25HC metabolism. The biosynthetic enzymes CH25H and CYP7B1 showed positive correlations with inflammatory markers, while HSD3B7, responsible for 7α25HC catabolism, demonstrated an inverse correlation. Unfortunately, in our studies the levels of 7α25HC were below the limit of quantification of our LC-MS method. Nevertheless, this pattern could suggest a regulatory response aimed at modulating 7α25HC levels during inflammation. These findings align with our previous work demonstrating the upregulation of these enzymes in DSS-induced colitis[13], and support the emerging role of 7α25HC in IBD. Indeed, previous studies have demonstrated that inflammatory diseases are characterized by increased levels of both 7α25HC and its receptor GPR183[15]. This tight regulation of 7α25HC is crucial in inflammatory contexts, particularly for directing immune cell migration and supporting lymphoid organ development[8, 15, 47, 48]. Interestingly, while we

ARTICLE IN PRESS

found changes in 7α25HC metabolic pathways, we found similar GPR183 expression between males and females (Supplementary Figure 2).

In vitro studies help to better isolate specific cellular responses. Several studies of in vitro cell systems, including the current study, have reported anti-inflammatory effects for 7α25HC, which are believed to be GPR183-dependent[49, 50]. However, in our experiments, the antagonists used (i.e. NIBR189 and GSK68753A) failed to antagonize the effects of 7α25HC. This could highlight that the timing of antagonist incubation appears to be critical. In vitro studies demonstrating clear antagonistic effects often used a pretreatment protocol with the antagonist NIBR189, followed by agonist exposure[49, 50]. A preincubation approach could represent a more strategic treatment plan for this receptor, allowing for more effective blockade of GPR183 prior to agonist challenge, but of course is less representative of a potential therapeutic intervention. In this study we also used PBMC isolated from healthy volunteers. Indeed, these circulating immune cells play crucial roles in IBD pathogenesis notably by being recruited to inflammatory sites. We found that these two stimuli differentially affected the expression of the oxysterol receptors, likely because they are activating different cell types within the PBMC population. In our working conditions, we found that 7α25HC had no effect neither on the LPS-induced nor on the PHA-induced PBMC activation. A limitation of this study lies in the use of PBMC from healthy donors. Yet our data support the interest of testing oxysterols effects on PBMC isolated from volunteers with IBD.

In our in vivo studies, administration of 7α25HC elicited modest effects on inflammatory markers in both sexes, with the most pronounced effect being reduced immune cell counts in mesenteric lymph nodes. This reduction could reflect 7α25HC-mediated cell migration from lymph nodes to other compartments, particularly the peritoneal cavity where the compound was administered. Wyss et

ARTICLE IN PRESS

al. reported that, in DSS-induced colitis, deletion of GPR183 or deletion of CH25H (resulting in decreased levels of 7α25HC, 25HC and 7α27HC) did not affect colitis severity[15]. The data we obtained using a pharmacological approach (i.e. the antagonist NIBR189) supports the findings of Wyss et al. as decreasing GPR183 signaling did not strongly impact DSS-induced colitis.

Comparing the data obtained with a pharmacological approach to those obtained using knockout models remains complex. The dosing regimen of 10 mg/kg of 7α25HC was used based on previous studies with related oxysterols[13]. However, this inherently resulted in higher levels compared to those found in untreated animals. In addition, the peritoneal administration route may create concentration gradients that are different from the more subtle endogenous gradients that normally guide immune cell positioning[8, 15]. Besides, oral administration could have provided different results than those we obtained following intraperitoneal dosing. Indeed, direct contact between the oxysterol and the damaged tissue could have enhanced local anti-inflammatory effects. However, contrary to other oxysterols (e.g. 5,6-epoxycholesterols and 7KC), 7α25HC is not reported as an important oxysterol present in the food and we thus opted for the intraperitoneal route in this study. These pharmacological considerations highlight the challenges in directly comparing studies that disrupt endogenous 7α25HC/GPR183 signaling through genetic approaches with those using exogenous ligand administration. Notably, our study is pioneering in its investigation of the pharmacological administration of both 7α25HC and its antagonist in this context[10, 26]. This complexity is further supported by the fact that GPR183 undergoes desensitization upon exposure to its ligand 7α25HC, which could attenuate subsequent chemotactic responses[51-53]. The dynamics of GPR183 signaling may therefore play a significant role in determining the overall inflammatory response. While more relevant to the clinic, as we pharmacologically interfered with the GPR183 axis, our study may have captured

ARTICLE IN PRESS

a different response compared to the effects of interfering with the 7α25HC/GPR183 axis observed in genetic deletion models[10, 26].

In conclusion, our study reveals important sex-specific differences in oxysterol metabolism and anti-inflammatory effects, with more pronounced responses in female colon explants compared to male counterparts. The coordinated regulation of enzymes involved in 7α25HC metabolism during inflammation, along with the sexually dimorphic correlation patterns observed with SULT2B1, suggest distinct regulatory mechanisms between males and females. Our in vivo administration of 7α25HC showed modest effects compared to in vitro findings, highlighting the complex nature of oxysterol signaling in inflammatory contexts. These findings collectively underscore the importance of considering sex as a biological variable in future experimental investigations of oxysterol metabolism and function in IBD.

ARTICLE IN PRESS

STATEMENTS AND DECLARATIONS

Funding statement: This work was supported by subsidies from the 'Fonds Spéciaux de Recherches' [FSR, UCLouvain] and from the Fonds de la Recherche Scientifique [FRS-FNRS]. HA was a research fellow from the FRS-FNRS and was also supported by an ARC grant (UCLouvain). JBE and PB are postdoctoral fellows from the FRS-FNRS. MA is a research associate of the FRS-FNRS.

Competing interest: The authors have no relevant financial or non-financial interests to disclose.

Authors contributions: HA: investigation and data analysis, Writing - original draft ; JBE: investigation and data analysis, Writing - review & editing; MR: investigation and data analysis, Writing - review & editing ; AL: investigation and data analysis, Writing - review & editing; PB: investigation and data analysis, Writing - review &

ARTICLE IN PRESS

editing; MA: supervision, investigation and data analysis, Writing - review & editing ; GGM: Conceptualization, Methodology, Supervision, investigation and data analysis, Writing - review & editing.

Data availability: All data are provided in this study, and raw data can be requested to the corresponding author.

Ethics approval: studies involving animals were approved by the UCLouvain's animal studies ethics committee (study agreements 2017/UCL/MD/024, 2021/UCL/MD/066 and 07-OTLADDB-2023-7, laboratory agreement LA1230635). Peripheral blood samples were obtained from healthy donors following informed consent. This study was approved by the ethics committee of UCLouvain and its affiliated hospital (cliniques universitaires Saint Luc) (2023/06JUI/252 - Belgian registration number: B4032023000052).

ARTICLE IN PRESS

ARTICLE IN PRESS

References

(1) Alhouayek, M.; Ameraoui, H.; Muccioli, G. G. Bioactive lipids in inflammatory bowel diseases – From pathophysiological alterations to therapeutic opportunities. *Biochimica et Biophysica Acta (BBA) - Molecular and Cell Biology of Lipids* **2021**, *1866* (2), 158854. DOI: https://doi.org/10.1016/j.bbalip.2020.158854.

(2) Mutemberezi, V.; Guillemot-Legris, O.; Muccioli, G. G. Oxysterols: From cholesterol metabolites to key mediators. *Progress in lipid research* **2016**, *64*, 152-169. DOI: 10.1016/j.plipres.2016.09.002 From NLM.

(3) Willinger, T. Oxysterols in intestinal immunity and inflammation. **2019**, *285* (4), 367-380. DOI: 10.1111/joim.12855.

(4) Liu, Y.; Wei, Z.; Ma, X.; Yang, X.; Chen, Y.; Sun, L.; Ma, C.; Miao, Q. R.; Hajjar, D. P.; Han, J.; et al. 25-Hydroxycholesterol activates the expression of cholesterol 25-hydroxylase in an LXR-dependent mechanism. *Journal of lipid research* **2018**, *59* (3), 439-451. DOI: 10.1194/jlr.M080440 From NLM.

(5) Mouzat, K.; Chudinova, A.; Polge, A.; Kantar, J.; Camu, W.; Raoul, C.; Lumbroso, S. Regulation of Brain Cholesterol: What Role Do Liver X Receptors Play in Neurodegenerative Diseases? *Int J Mol Sci* **2019**, *20* (16). DOI: 10.3390/ijms20163858 From NLM.

(6) Ning, Y.; Kim, J. K.; Min, H. K.; Ren, S. Cholesterol metabolites alleviate injured liver function and decrease mortality in an LPS-induced mouse model. *Metabolism* **2017**, *71*, 83-93. DOI: 10.1016/j.metabol.2016.12.007 From NLM.

(7) Bottemanne, P.; Paquot, A.; Ameraoui, H.; Guillemot-Legris, O.; Alhouayek, M.; Muccioli, G. G. 25-Hydroxycholesterol metabolism is altered by lung inflammation, and its local administration modulates lung inflammation in mice. *FASEB journal : official publication of the Federation of American Societies for Experimental Biology* **2021**, *35* (4), e21514. DOI: 10.1096/fj.202002555R From NLM.

(8) Emgård, J.; Kammoun, H.; García-Cassani, B.; Chesné, J.; Parigi, S. M.; Jacob, J.-M.; Cheng, H.-W.; Evren, E.; Das, S.; Czarnewski, P.; et al. Oxysterol Sensing through the Receptor GPR183 Promotes the Lymphoid-Tissue-Inducing Function of Innate Lymphoid Cells and Colonic Inflammation. *Immunity* **2018**, *48* (1), 120-132.e128. DOI: https://doi.org/10.1016/j.immuni.2017.11.020.

ARTICLE IN PRESS

(9) Jia, J.; Conlon, T. M.; Sarker, R. S.; Taşdemir, D.; Smirnova, N. F.; Srivastava, B.; Verleden, S. E.; Güneş, G.; Wu, X.; Prehn, C.; et al. Cholesterol metabolism promotes B-cell positioning during immune pathogenesis of chronic obstructive pulmonary disease. *EMBO Mol Med* **2018**, *10* (5), e8349. DOI: 10.15252/emmm.201708349 PubMed.

(10) Foo, C. X.; Bartlett, S.; Chew, K. Y.; Ngo, M. D.; Bielefeldt-Ohmann, H.; Arachchige, B. J.; Matthews, B.; Reed, S.; Wang, R.; Smith, C.; et al. GPR183 antagonism reduces macrophage infiltration in influenza and SARS-CoV-2 infection. *Eur Respir J* **2023**, *61* (3). DOI: 10.1183/13993003.01306-2022 From NLM.

(11) Barington, L.; Christensen, L. v. V.; Pedersen, K. K.; Niss Arfelt, K.; Roumain, M.; Jensen, K. H. R.; Kjær, V. M. S.; Daugvilaite, V.; Kearney, J. F.; Christensen, J. P.; et al. GPR183 Is Dispensable for B1 Cell Accumulation and Function, but Affects B2 Cell Abundance, in the Omentum and Peritoneal Cavity. **2022**, *11* (3), 494.

(12) Soroosh, P.; Wu, J.; Xue, X.; Song, J.; Sutton, S. W.; Sablad, M.; Yu, J.; Nelen, M. I.; Liu, X.; Castro, G.; et al. Oxysterols are agonist ligands of RORγt and drive Th17 cell differentiation. *Proceedings of the National Academy of Sciences of the United States of America* **2014**, *111* (33), 12163-12168. DOI: 10.1073/pnas.1322807111 From NLM.

(13) Guillemot-Legris, O.; Mutemberezi, V.; Buisseret, B.; Paquot, A.; Palmieri, V.; Bottemanne, P.; Lemaire, J.; Rahier, J. F.; Alhouayek, M.; Muccioli, G. G. Colitis Alters Oxysterol Metabolism and is Affected by 4beta-Hydroxycholesterol Administration. *Journal of Crohn's & colitis* **2019**, *13* (2), 218-229. DOI: 10.1093/ecco-jcc/jjy157 From NLM.

(14) Iwamoto, J.; Saito, Y.; Honda, A.; Miyazaki, T.; Ikegami, T.; Matsuzaki, Y. Bile acid malabsorption deactivates pregnane X receptor in patients with Crohn's disease. *Inflammatory bowel diseases* **2013**, *19* (6), 1278-1284. DOI: 10.1097/MIB.0b013e318281f423 From NLM.

(15) Wyss, A.; Raselli, T.; Perkins, N.; Ruiz, F.; Schmelczer, G.; Klinke, G.; Moncsek, A.; Roth, R.; Spalinger, M. R.; Hering, L.; et al. The EBI2-oxysterol axis promotes the development of intestinal lymphoid structures and colitis. *Mucosal Immunology* **2019**, *12* (3), 733-745. DOI: 10.1038/s41385-019-0140-x.

ARTICLE IN PRESS

(16) Gargiulo, S.; Gamba, P.; Testa, G.; Rossin, D.; Biasi, F.; Poli, G.; Leonarduzzi, G. Relation between TLR4/NF-κB signaling pathway activation by 27-hydroxycholesterol and 4-hydroxynonenal, and atherosclerotic plaque instability. **2015**, *14* (4), 569-581. DOI: https://doi.org/10.1111/acel.12322.

(17) Ma, Y.; Xu, L.; Rodriguez-Agudo, D.; Li, X.; Heuman, D. M.; Hylemon, P. B.; Pandak, W. M.; Ren, S. 25-Hydroxycholesterol-3-sulfate regulates macrophage lipid metabolism via the LXR/SREBP-1 signaling pathway. *Am J Physiol Endocrinol Metab* **2008**, *295* (6), E1369-1379. DOI: 10.1152/ajpendo.90555.2008 From NLM.

(18) Xu, L.; Shen, S.; Ma, Y.; Kim, J.; Rodriguez-Agudo, D.; Heuman, D.; Hylemon, P.; Pandak, W.; Ren, S. 25-Hydroxycholesterol-3-sulfate attenuates inflammatory response via PPAR signaling in human THP-1 macrophages. *American journal of physiology. Endocrinology and metabolism* **2012**, *302*, E788-799. DOI: 10.1152/ajpendo.00337.2011.

(19) A-González, N.; Castrillo, A. Liver X receptors as regulators of macrophage inflammatory and metabolic pathways. *Biochimica et Biophysica Acta (BBA) - Molecular Basis of Disease* **2011**, *1812* (8), 982-994. DOI: https://doi.org/10.1016/j.bbadis.2010.12.015.

(20) Wu, J.; McDuffie, J. E.; Song, J.; Harris, M. C.; Raymond, H.; Chen, Y.; Nguyen, L.; Nguyen, S.; Kanerva, J.; McAllister, H. M.; et al. LC/MS/MS Profiling of Tissue Oxysterols and its Application in Dextran Sodium Sulphate Induced Mouse Colitis Models. *Current topics in medicinal chemistry* **2017**, *17* (24), 2781-2790. DOI: 10.2174/1568026617666170713165519 From NLM.

(21) Sheng, N.; Ma, Z.; Zhou, Y.; Xu, J.; Gao, Y.; Fu, X. Y. Cholesterol 25-hydroxylase protects against experimental colitis in mice by modulating epithelial gut barrier function. *Scientific reports* **2020**, *10* (1), 14246. DOI: 10.1038/s41598-020-71198-1 From NLM.

(22) McNamee, E. N.; Masterson, J. C.; Jedlicka, P.; McManus, M.; Grenz, A.; Collins, C. B.; Nold, M. F.; Nold-Petry, C.; Bufler, P.; Dinarello, C. A.; et al. Interleukin 37 expression protects mice from colitis. *Proceedings of the National Academy of Sciences of the United States of America* **2011**, *108* (40), 16711-16716. DOI: 10.1073/pnas.1111982108 From NLM.

ARTICLE IN PRESS

(23) Pleguezuelos-Manzano, C.; Puschhof, J.; van den Brink, S.; Geurts, V.; Beumer, J.; Clevers, H. Establishment and Culture of Human Intestinal Organoids Derived from Adult Stem Cells. *Curr Protoc Immunol* **2020**, *130* (1), e106. DOI: 10.1002/cpim.106 From NLM.

(24) Alhouayek, M.; Bottemanne, P.; Subramanian, K. V.; Lambert, D. M.; Makriyannis, A.; Cani, P. D.; Muccioli, G. G. N-Acylethanolamine-hydrolyzing acid amidase inhibition increases colon N-palmitoylethanolamine levels and counteracts murine colitis. *FASEB journal : official publication of the Federation of American Societies for Experimental Biology* **2015**, *29* (2), 650-661. DOI: 10.1096/fj.14-255208 From NLM.

(25) Alhouayek, M.; Buisseret, B.; Paquot, A.; Guillemot-Legris, O.; Muccioli, G. G. The endogenous bioactive lipid prostaglandin D(2)-glycerol ester reduces murine colitis via DP1 and PPARγ receptors. *FASEB journal : official publication of the Federation of American Societies for Experimental Biology* **2018**, *32* (9), 5000-5011. DOI: 10.1096/fj.201701205R From NLM.

(26) Tang, J.; Shi, Y.; Zhan, L.; Qin, C. Downregulation of GPR183 on infection restricts the early infection and intracellular replication of mycobacterium tuberculosis in macrophage. *Microb Pathog* **2020**, *145*, 104234. DOI: 10.1016/j.micpath.2020.104234 From NLM.

(27) Kämpfer, A. A. M.; Urbán, P.; Gioria, S.; Kanase, N.; Stone, V.; Kinsner-Ovaskainen, A. Development of an in vitro co-culture model to mimic the human intestine in healthy and diseased state. *Toxicology in Vitro* **2017**, *45*, 31-43. DOI: https://doi.org/10.1016/j.tiv.2017.08.011.

(28) Viennois, E.; Chen, F.; Laroui, H.; Baker, M. T.; Merlin, D. Dextran sodium sulfate inhibits the activities of both polymerase and reverse transcriptase: lithium chloride purification, a rapid and efficient technique to purify RNA. *BMC Research Notes* **2013**, *6* (1), 360. DOI: 10.1186/1756-0500-6-360.

(29) Mutemberezi, V.; Masquelier, J.; Guillemot-Legris, O.; Muccioli, G. G. Development and validation of an HPLC-MS method for the simultaneous quantification of key oxysterols, endocannabinoids, and ceramides: variations in metabolic syndrome. *Anal Bioanal Chem* **2016**, *408* (3), 733-745. DOI: 10.1007/s00216-015-9150-z From NLM.

ARTICLE IN PRESS

(30) Mutemberezi, V.; Buisseret, B.; Masquelier, J.; Guillemot-Legris, O.; Alhouayek, M.; Muccioli, G. G. Oxysterol levels and metabolism in the course of neuroinflammation: insights from in vitro and in vivo models. *Journal of Neuroinflammation* **2018**, *15* (1), 74. DOI: 10.1186/s12974-018-1114-8.

(31) Roumain, M.; Guillemot-Legris, O.; Ameraoui, H.; Alhouayek, M.; Muccioli, G. G. Identification and in vivo detection of side-chain hydroxylated metabolites of 4β-hydroxycholesterol. *J Steroid Biochem Mol Biol* **2023**, *234*, 106376. DOI: 10.1016/j.jsbmb.2023.106376 From NLM.

(32) Eichele, D. D.; Kharbanda, K. K. Dextran sodium sulfate colitis murine model: An indispensable tool for advancing our understanding of inflammatory bowel diseases pathogenesis. *World journal of gastroenterology* **2017**, *23* (33), 6016-6029. DOI: 10.3748/wjg.v23.i33.6016 From NLM.

(33) Chassaing, B.; Aitken, J. D.; Malleshappa, M.; Vijay-Kumar, M. Dextran sulfate sodium (DSS)-induced colitis in mice. *Curr Protoc Immunol* **2014**, *104*, 15.25.11-15.25.14. DOI: 10.1002/0471142735.im1525s104 From NLM.

(34) Greuter, T.; Manser, C.; Pittet, V.; Vavricka, Stephan R.; Biedermann, L.; on behalf of Swiss IBDnet, a. o. w. g. o. t. S. S. o. G. Gender Differences in Inflammatory Bowel Disease. *Digestion* **2020**, *101* (Suppl. 1), 98-104. DOI: 10.1159/000504701 (acccessed 1/18/2025).

(35) Yi, T.; Wang, X.; Kelly, L. M.; An, J.; Xu, Y.; Sailer, A. W.; Gustafsson, J. A.; Russell, D. W.; Cyster, J. G. Oxysterol gradient generation by lymphoid stromal cells guides activated B cell movement during humoral responses. *Immunity* **2012**, *37* (3), 535-548. DOI: 10.1016/j.immuni.2012.06.015 From NLM.

(36) Guillemot-Legris, O.; Muccioli, G. G. The oxysterome and its receptors as pharmacological targets in inflammatory diseases. *British journal of pharmacology* **2022**, *179* (21), 4917-4940. DOI: 10.1111/bph.15479 From

(37) Lawlor, N.; Nehar-Belaid, D.; Grassmann, J. D. S.; Stoeckius, M.; Smibert, P.; Stitzel, M. L.; Pascual, V.; Banchereau, J.; Williams, A.; Ucar, D. Single Cell Analysis of Blood Mononuclear Cells Stimulated Through Either LPS or Anti-CD3 and Anti-CD28. *Frontiers in immunology* **2021**, *Volume 12 - 2021*, Original Research. DOI: 10.3389/fimmu.2021.636720.

ARTICLE IN PRESS

(38) Lorbek, G.; Perše, M.; Horvat, S.; Björkhem, I.; Rozman, D. Sex differences in the hepatic cholesterol sensing mechanisms in mice. *Molecules* **2013**, *18* (9), 11067-11085. DOI: 10.3390/molecules180911067 From NLM.

(39) Guillemot-Legris, O.; Mutemberezi, V.; Muccioli, G. G. Oxysterols in Metabolic Syndrome: From Bystander Molecules to Bioactive Lipids. *Trends in molecular medicine* **2016**, *22* (7), 594-614. DOI: 10.1016/j.molmed.2016.05.006 From NLM.

(40) Yang, L.; Li, Y.; Hong, H.; Chang, C. W.; Guo, L. W.; Lyn-Cook, B.; Shi, L.; Ning, B. Sex Differences in the Expression of Drug-Metabolizing and Transporter Genes in Human Liver. *J Drug Metab Toxicol* **2012**, *3* (3), 1000119. DOI: 10.4172/2157-7609.1000119 From NLM.

(41) Raselli, T.; Wyss, A.; Gonzalez Alvarado, M. N.; Weder, B.; Mamie, C.; Spalinger, M. R.; Van Haaften, W. T.; Dijkstra, G.; Sailer, A. W.; Imenez Silva, P. H.; et al. The Oxysterol Synthesising Enzyme CH25H Contributes to the Development of Intestinal Fibrosis. *Journal of Crohn's & colitis* **2019**, *13* (9), 1186-1200. DOI: 10.1093/ecco-jcc/jjz039 From NLM.

(42) Rustgi, S. D.; Kayal, M.; Shah, S. C. Sex-based differences in inflammatory bowel diseases: a review. **2020**, *13*, 1756284820915043. DOI: 10.1177/1756284820915043.

(43) Umetani, M.; Shaul, P. W. 27-Hydroxycholesterol: the first identified endogenous SERM. *Trends Endocrinol Metab* **2011**, *22* (4), 130-135. DOI: 10.1016/j.tem.2011.01.003 From NLM.

(44) Jakobsson, T.; Vedin, L. L.; Hassan, T.; Venteclef, N.; Greco, D.; D'Amato, M.; Treuter, E.; Gustafsson, J.; Steffensen, K. R. The oxysterol receptor LXRβ protects against DSS- and TNBS-induced colitis in mice. *Mucosal Immunol* **2014**, *7* (6), 1416-1428. DOI: 10.1038/mi.2014.31 From NLM.

(45) Goodman, W. A.; Havran, H. L.; Quereshy, H. A.; Kuang, S.; De Salvo, C.; Pizarro, T. T. Estrogen Receptor α Loss-of-Function Protects Female Mice From DSS-Induced Experimental Colitis. *Cellular and molecular gastroenterology and hepatology* **2017**, *5* (4), 630-633.e631. DOI: 10.1016/j.jcmgh.2017.12.003 PubMed.

ARTICLE IN PRESS

(46) Stiles, A. R.; McDonald, J. G.; Bauman, D. R.; Russell, D. W. CYP7B1: one cytochrome P450, two human genetic diseases, and multiple physiological functions. *The Journal of biological chemistry* **2009**, *284* (42), 28485-28489. DOI: 10.1074/jbc.R109.042168 From NLM.

(47) Yi, T.; Wang, X.; Kelly, Lisa M.; An, J.; Xu, Y.; Sailer, Andreas W.; Gustafsson, J.-A.; Russell, David W.; Cyster, Jason G. Oxysterol Gradient Generation by Lymphoid Stromal Cells Guides Activated B Cell Movement during Humoral Responses. *Immunity* **2012**, *37* (3), 535-548. DOI: https://doi.org/10.1016/j.immuni.2012.06.015.

(48) Jia, J.; Conlon, T. M.; Sarker, R. S.; Taşdemir, D.; Smirnova, N. F.; Srivastava, B.; Verleden, S. E.; Güneş, G.; Wu, X.; Prehn, C.; et al. Cholesterol metabolism promotes B-cell positioning during immune pathogenesis of chronic obstructive pulmonary disease. *EMBO Mol Med* **2018**, *10* (5). DOI: 10.15252/emmm.201708349 From NLM.

(49) Rutkowska, A.; Shimshek, D. R.; Sailer, A. W.; Dev, K. K. EBI2 regulates pro-inflammatory signalling and cytokine release in astrocytes. *Neuropharmacology* **2018**, *133*, 121-128. DOI: https://doi.org/10.1016/j.neuropharm.2018.01.029.

(50) Bartlett, S.; Gemiarto, A. T.; Ngo, M. D.; Sajiir, H.; Hailu, S.; Sinha, R.; Foo, C. X.; Kleynhans, L.; Tshivhula, H.; Webber, T.; et al. GPR183 Regulates Interferons, Autophagy, and Bacterial Growth During Mycobacterium tuberculosis Infection and Is Associated With TB Disease Severity. **2020**, *11*, Original Research. DOI: 10.3389/fimmu.2020.601534.

(51) Liu, C.; Yang, X. V.; Wu, J.; Kuei, C.; Mani, N. S.; Zhang, L.; Yu, J.; Sutton, S. W.; Qin, N.; Banie, H.; et al. Oxysterols direct B-cell migration through EBI2. *Nature* **2011**, *475* (7357), 519-523. DOI: 10.1038/nature10226 From NLM.

(52) Kjær, V. M. S.; Daugvilaite, V.; Stepniewski, T. M.; Madsen, C. M.; Jørgensen, A. S.; Bhuskute, K. R.; Inoue, A.; Ulven, T.; Benned-Jensen, T.; Hjorth, S. A.; et al. Migration mediated by the oxysterol receptor GPR183 depends on arrestin coupling but not receptor internalization. *Sci Signal* **2023**, *16* (779), eabl4283. DOI: 10.1126/scisignal.abl4283 From NLM.

(53) Braden, K.; Campolo, M.; Li, Y.; Chen, Z.; Doyle, T. M.; Giancotti, L. A.; Esposito, E.; Zhang, J.; Cuzzocrea, S.; Arnatt, C. K.; et al. Activation of GPR183 by 7α,25-

ARTICLE IN PRESS

Dihydroxycholesterol Induces Behavioral Hypersensitivity through Mitogen-Activated Protein Kinase and Nuclear Factor-κB. *The Journal of pharmacology and experimental therapeutics* **2022**, *383* (2), 172-181. DOI: 10.1124/jpet.122.001283 From NLM.

ARTICLE IN PRESS

Figure 1. DSS-induced colitis differently alters inflammatory markers and oxysterol levels in the colon tissue of male and female mice. C57BL/6 male and female mice received 5% DSS in the drinking water for 5 days, followed by water for 2 days to induce colitis. **(A)** Colon weight-to-length ratio. **(B)** Myeloperoxidase (MPO) activity in the colon, expressed relative to the activity measured in male control (veh.) mice. **(C)** Levels of the inflammatory marker IL-6 measured by ELISA. **(D)** mRNA expression of inflammation markers measured by RT-qPCR, with RPL19 used as a reference gene and expressed as percentage of the male control (veh.) condition. **(E)** Oxysterols were quantified by HPLC-MS and results are expressed in pmol per g of colon tissue. **(F)** Principal component analysis (PCA) for colon oxysterol levels. **(G)** Correlation heatmaps showing the relationships between colon oxysterol levels and colon inflammatory parameters in male and female mice. Data are presented as mean ± SEM (N=8 mice per group). *P < 0.05, **P < 0.01, ***P < 0.001, ****P < 0.0001 vs. respective vehicle (veh.); $$P < 0.01, $$$P < 0.001 for female vs. male veh., #P < 0.05, ##P < 0.01, ###P < 0.001 for female vs. male DSS.

Figure 2. DSS-induced colitis alters oxysterol levels in the plasma differently between male and female mice. Colitis was induced in male and female C57BL/6 mice as described in figure 1. (**A**) Oxysterols were quantified by HPLC-MS and the results expressed as pmol/µl of plasma. (**B**) Principal component analysis (PCA) plot of plasma oxysterol levels. Results are presented as mean ± SEM (N=8 mice per group). *P < 0.05, **P < 0.01, ****P < 0.0001 vs. respective vehicle (veh.); $P < 0.05, $$P < 0.01, $$$P < 0.001 for female vs. male veh.; #P < 0.05, ##P < 0.01 for female vs. male DSS.

Figure 3. 25HC3S and 7α25HC decreased pro-inflammatory cytokine production by female, but not male, colon explants from mice with DSS-induced colitis. The colons from male (**A**) and female (**B**) DSS-treated mice were prepared as 400 µm slices and treated with oxysterols (1 or 10 µM) or vehicle (DMSO 0.1%; veh.). MCP-1 and IL-6 production was measured by ELISA in the culture medium after 8h of incubation. Results are expressed as percentage of the vehicle condition. Data are presented as mean ± SEM (N=3, in triplicates). *$P <$ 0.05, **P < 0.01 vs. veh.

Figure 4. Ex-vivo treatment of colon organoids with oxysterols. Colon organoids were prepared from the colon of healthy male mice and subsequently activated by incubating them with LPS (1 µg/mL) and INFγ (10 ng/mL). The organoids were co-incubated with the oxysterols (1 µM and 10 µM) or vehicle (DMSO, 0.1%) for 24h. (**A**) mRNA expression of inflammation markers measured by RT-qPCR, with RPL19 used as a reference gene. (**B**) TNF-α levels were measured by ELISA in the organoid culture media. In all the experiments an unstimulated condition was performed in which the organoids were incubated with DMSO 0.1% (veh.) in the absence of LPS and IFNγ. The results are expressed relative to the vehicle-LPS+IFNγ treated condition and are shown as mean ± SEM (N=4 in triplicates). *P < 0.05, ***P < 0.001 vs. LPS+IFNγ.

Figure 5. Oxysterols decrease cytokine production by activated THP-1-derived macrophages. THP-1 monocytes were differentiated with PMA (50 nM) for 48h followed by 24h plain media. (**A**) Differentiated THP-1 cells were subsequently activated using LPS (100 ng/mL) and IFNγ (10 ng/mL) in the presence of the oxysterols (1 µM and 10 µM) or vehicle (DMSO, 0.1%, veh.) for 8h. (**B**) The mRNA expression of oxysterol receptors was assessed by RT-qPCR, with RPL19 used as a reference gene, in undifferentiated THP-1 cells and in PMA-differentiated THP-1 cells activated (LPS + IFNγ) and nonactivated (veh.). The left Y-axis represents the difference in threshold cycle between the target and the reference (RPL19) gene (ΔCt). The right Y-axis represents the values as percentage respective to the non-activated PMA-differentiated condition. (**C**) Differentiated THP-1 cells were treated with vehicle (DMSO, 0.2%), 25-hydroxycholesterol-3-sulfate (25HC3S), the PPARγ antagonist T0070907 (3µM) or a combination of both. (**D**) Differentiated THP-1 cells were treated with vehicle (DMSO, 0.2%), 7α,25-dihydroxycholesterol (7α25HC), the GPR183 receptor antagonists NIBR189 (10 µM) or GSK682753A (10 µM) or a combination of the oxysterol with a GPR183 antagonist. In **A, C and D**, IL-6 and TNF-α levels were measured in the culture medium after 8h of incubation and expressed relative to the veh.-LPS+IFNγ activated condition. Data are shown as mean ± SEM (N=3 in triplicates). *$P < 0.05$, **$P < 0.01$, ***$P < 0.001$, ****$P < 0.0001$ vs. veh.-LPS+IFNγ (A, C and D) or PMA-non-activated (veh.-PMA) in (D); #P < 0.05 vs. LPS+IFNγ+7α25HC.

Figure 6. Treatment of PBMC with oxysterols. PMBC were isolated from freshly collected blood from healthy volunteers. (**A**) PBMC were activated with LPS (1 µg/ml) and co-treated with oxysterols (1 µM and 10 µM) or vehicle (DMSO, 0.1%, veh.) for 8h. (**B**-**C**) PBMC were activated with PHA (5 µg/ml) for 48h and treated with oxysterols (1 µM and 10 µM) or vehicle (DMSO, 0.1%, veh.) during the last 24h. TNF-α and IL-6 secretion in culture media was measured by ELISA. IFNγ and IL-13 mRNA expression was assessed by RT-qPCR with RPL19 used as a reference gene. Results are expressed as a percentage of the vehicle-treated LPS-activated (A) or PHA-activated (B-C) conditions and are shown as mean ± SEM (N=7 in triplicates). *P < 0.05, ***P < 0.001, ****P < 0.0001 vs. PHA-untreated.

ARTICLE IN PRESS

Figure 7. 7α25HC treatment in male or female mice does not affect macroscopic and histological hallmarks of DSS induced colitis. C57BL/6 male (**A**, **C**-**D**) and female (**B**, **E**-**F**) mice received 5% DSS in the drinking water for 5 days, followed by water for 2 days to induce colitis. The control group (veh.) received normal drinking water throughout the experiment. DSS-treated mice received 7α25HC (10 mg/kg, i.p.), NIBR189 (10 mg/kg, i.p.), a combination of 7α25HC and NIBR189 (10 mg/kg each, i.p.), or vehicle daily starting on the day of addition of DSS in the water. Body weight change in male (**A**) and female mice (**B**) over the course of the experiment. Colon weight/length ratio, spleen weight and caecal content in male (**C**) and female (**E**) mice. Histological score blindly established following hematoxylin and eosin staining of the colon in male (**D**) and female (**F**) mice. Results are shown as mean ± SEM (N=8 mice/group). *$P < 0.05$, **$P < 0.01$, **** $P< 0.0001$ vs. vehicle-DSS treated group.

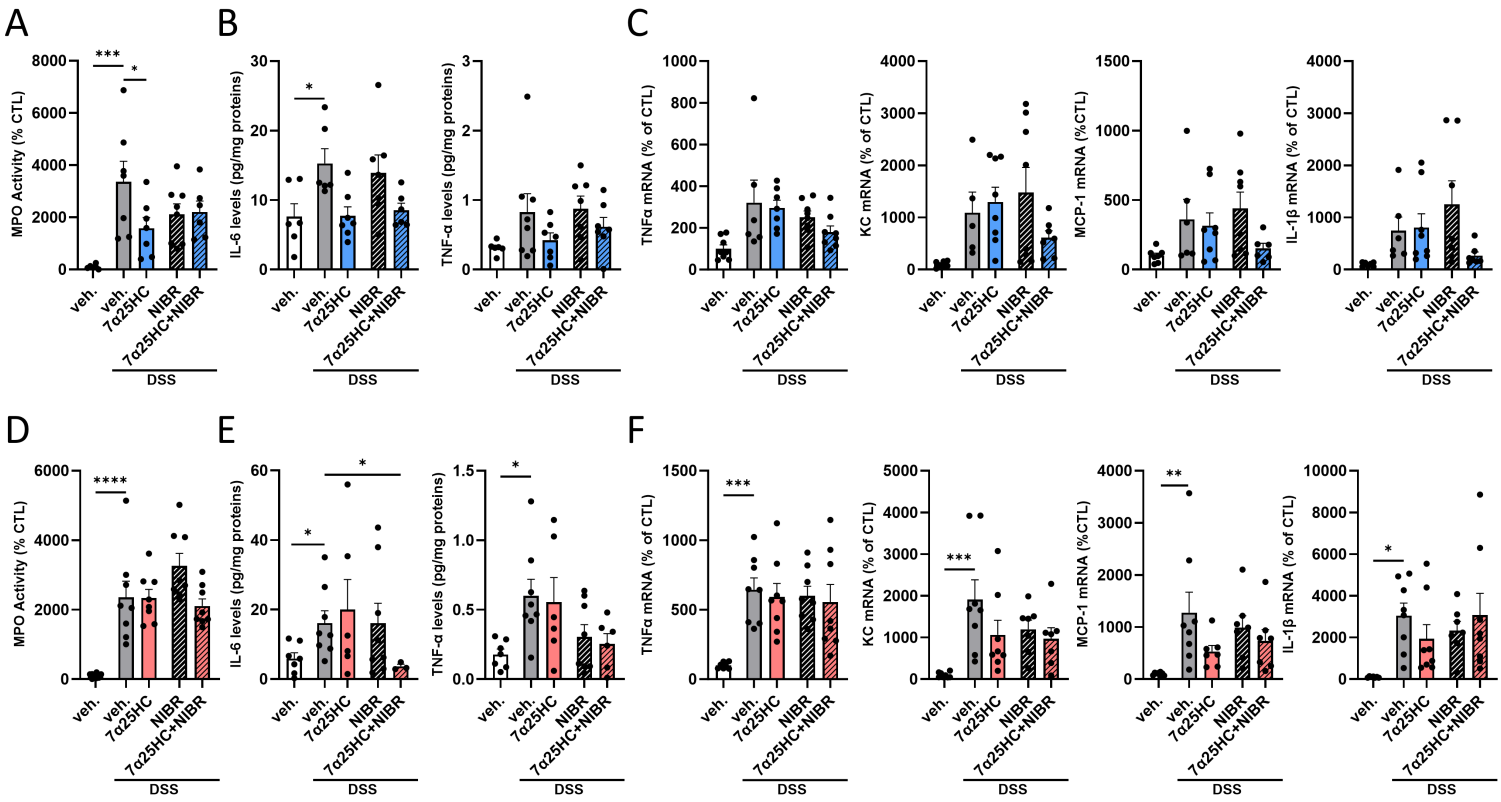
Figure 8. Inflammatory markers in the colon upon 7α25HC treatment in DSS-induced colitis. Mice were treated as described in Figure 7. Myeloperoxidase (MPO) activity in the colon of male **(A)** and female **(D)** mice is expressed in percentage of the veh. group not receiving DSS (CTL). IL-6 and TNF-

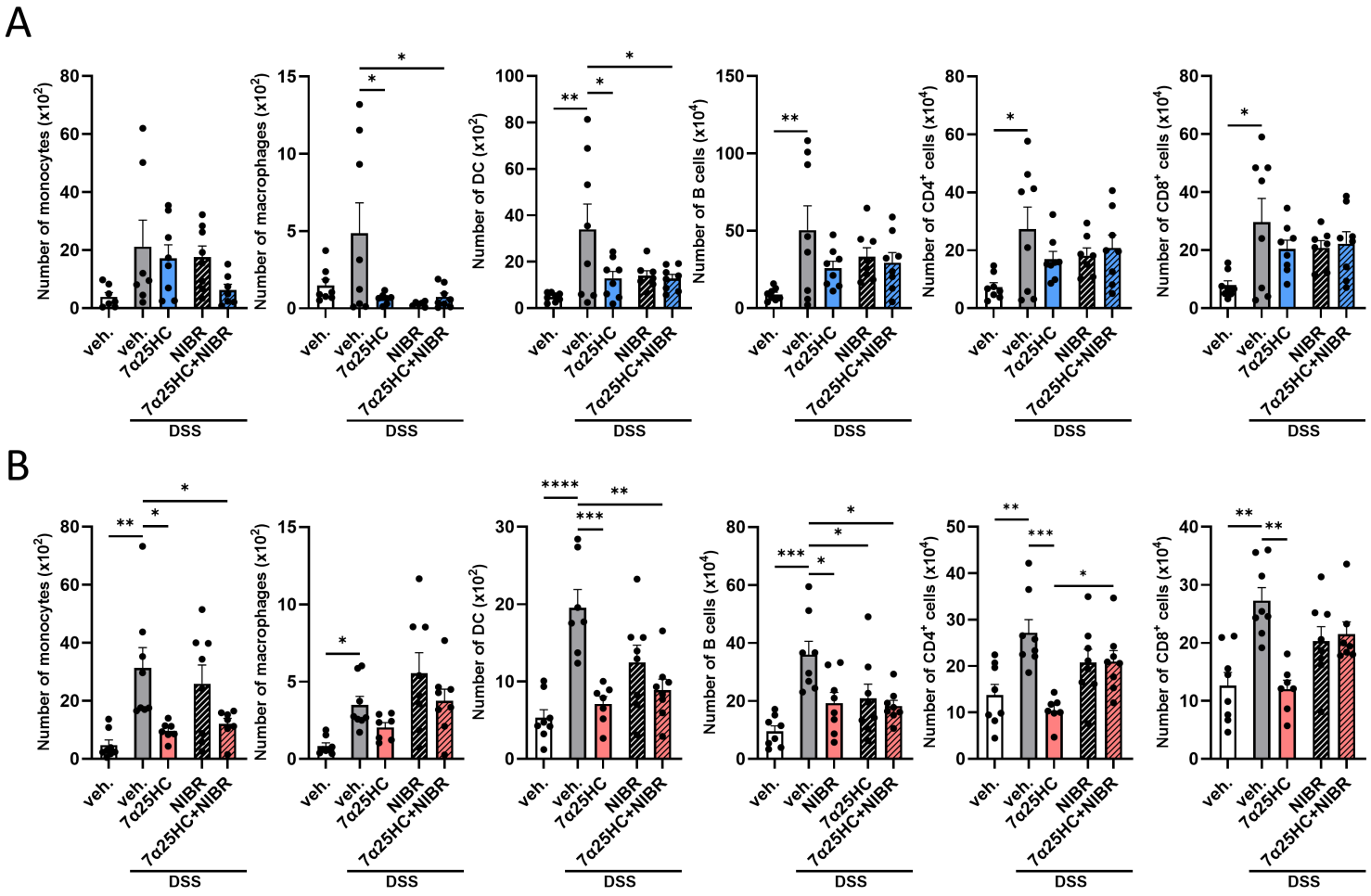
ARTICLE IN PRESS

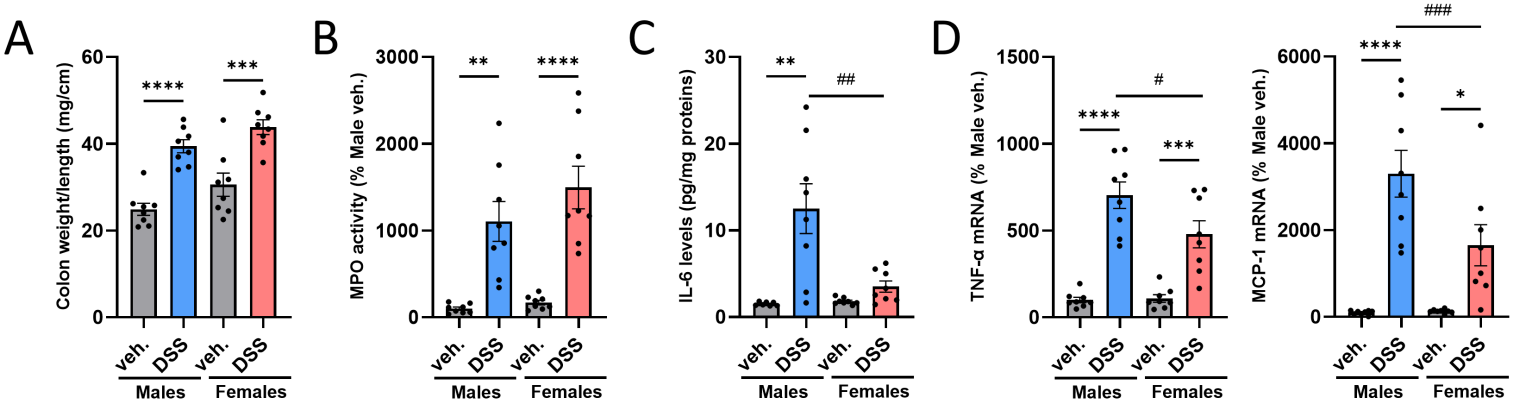
α levels were measured by ELISA in male **(B)** and female **(E)** mice colon homogenates. mRNA expression of proinflammatory cytokines assessed by RT-qPCR with RPL19 used as a reference gene in the colon of male **(C)** and female **(F)** mice. Data are expressed in percentage of the veh. group not receiving DSS (CTL). Results are shown as mean ± SEM (N=8 mice/group). *$P < 0.05$, **$P < 0.01$, ***$P < 0.001$, **** $P< 0.0001$ vs. vehicle-DSS treated group.

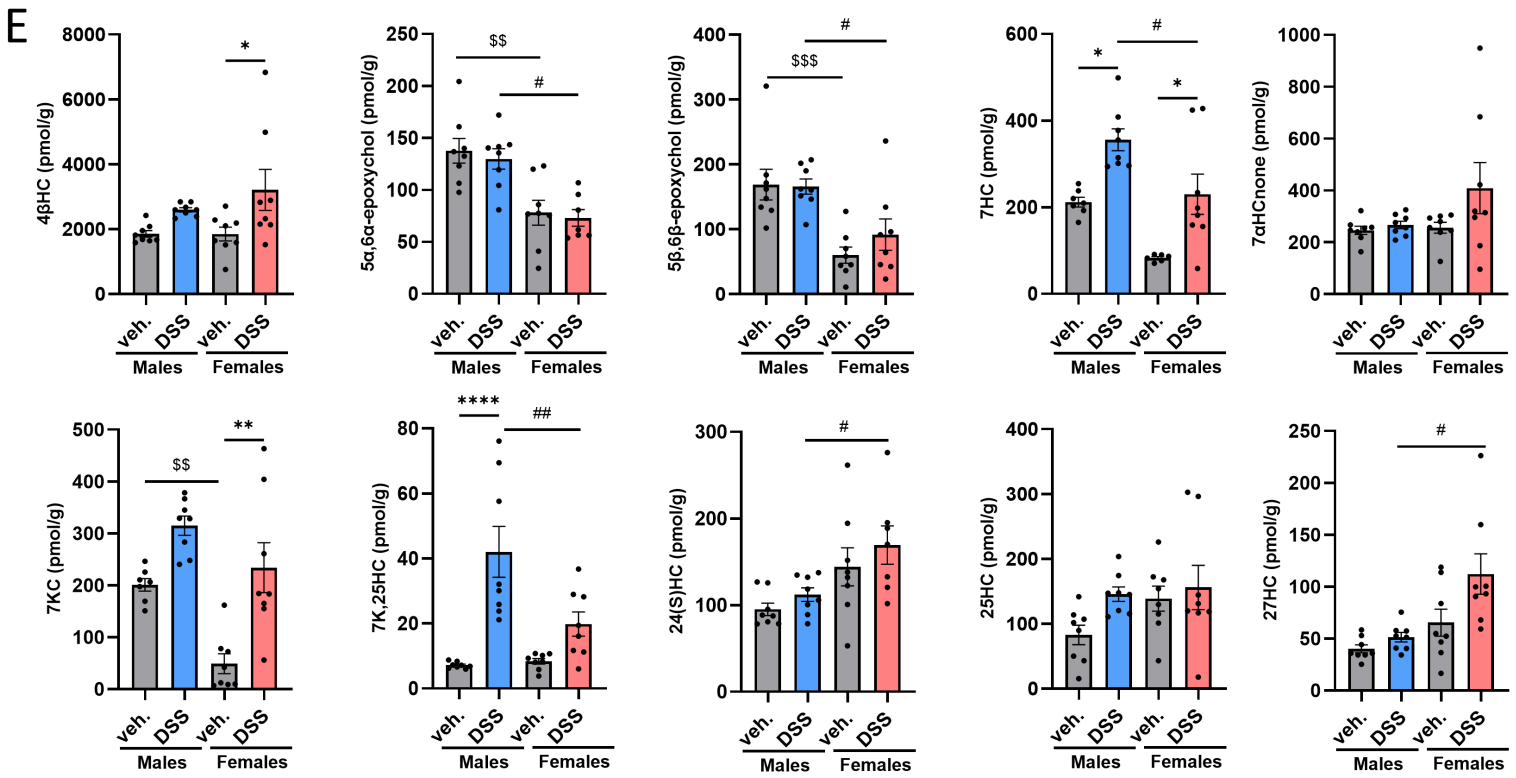
Figure 9. 7α25HC treatment modulates the immune cell populations in the mesenteric lymph nodes of DSS-induced colitis. Flow cytometry analysis of immune cell populations in the mesenteric lymph nodes from male (**A**) and female (**B**) mice. Mice were treated as described in Figure 7. The quantification of monocytes (CD45+/CD11b+/Ly6C+), dendritic cells (CD45+/CD11b+/Ly6C-/CD11c+), macrophages (CD45+/CD11b+/Ly6C-/CD11c-/F4-80+), B cells (CD45+/CD11b-/CD19+), CD4 T cells (CD45+/CD11b-/CD19-/CD4+/CD8-), and CD8 T cells (CD45+/CD11b-/CD19-/CD4-/CD8+) was obtained using the gating approach illustrated in SI figure 6. Data are expressed as the number of total cells in two lymph nodes. Results are shown as means ± SEM (N=8 mice/group). *$P < 0.05$, **$P < 0.01$, ***$P < 0.001$ vs. vehicle-DSS treated group.

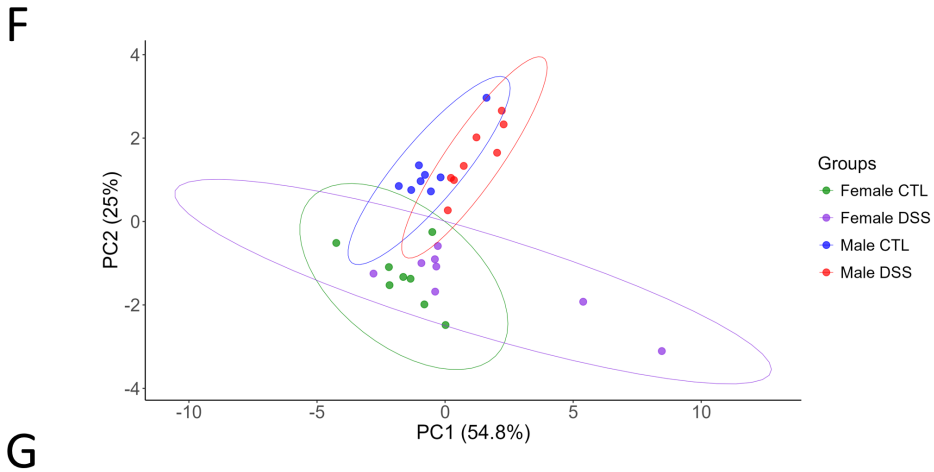
ARTICLE IN PRESS


A
B
C
D
E
F
MPO Activity (% CTL)
IL-6 levels (pg/mg proteins)
TNF-α levels (pg/mg proteins)
TNFα mRNA (% of CTL)
KC mRNA (% of CTL)
MCP-1 mRNA (%CTL)
IL-1β mRNA (% of CTL)
veh.
veh.
7α25HC
NIBR
7α25HC+NIBR
DSS


A
Number of monocytes (x10²)
Number of macrophages (x10²)
Number of DC (x10²)
Number of B cells (x10⁴)
Number of CD4⁺ cells (x10⁴)
Number of CD8⁺ cells (x10⁴)
veh.
veh.
7α25HC
NIBR
7α25HC+NIBR
DSS
B
Number of monocytes (x10²)
Number of macrophages (x10²)
Number of DC (x10²)
Number of B cells (x10⁴)
Number of CD4⁺ cells (x10⁴)
Number of CD8⁺ cells (x10⁴)
veh.
veh.
7α25HC
NIBR
7α25HC+NIBR
DSS







G

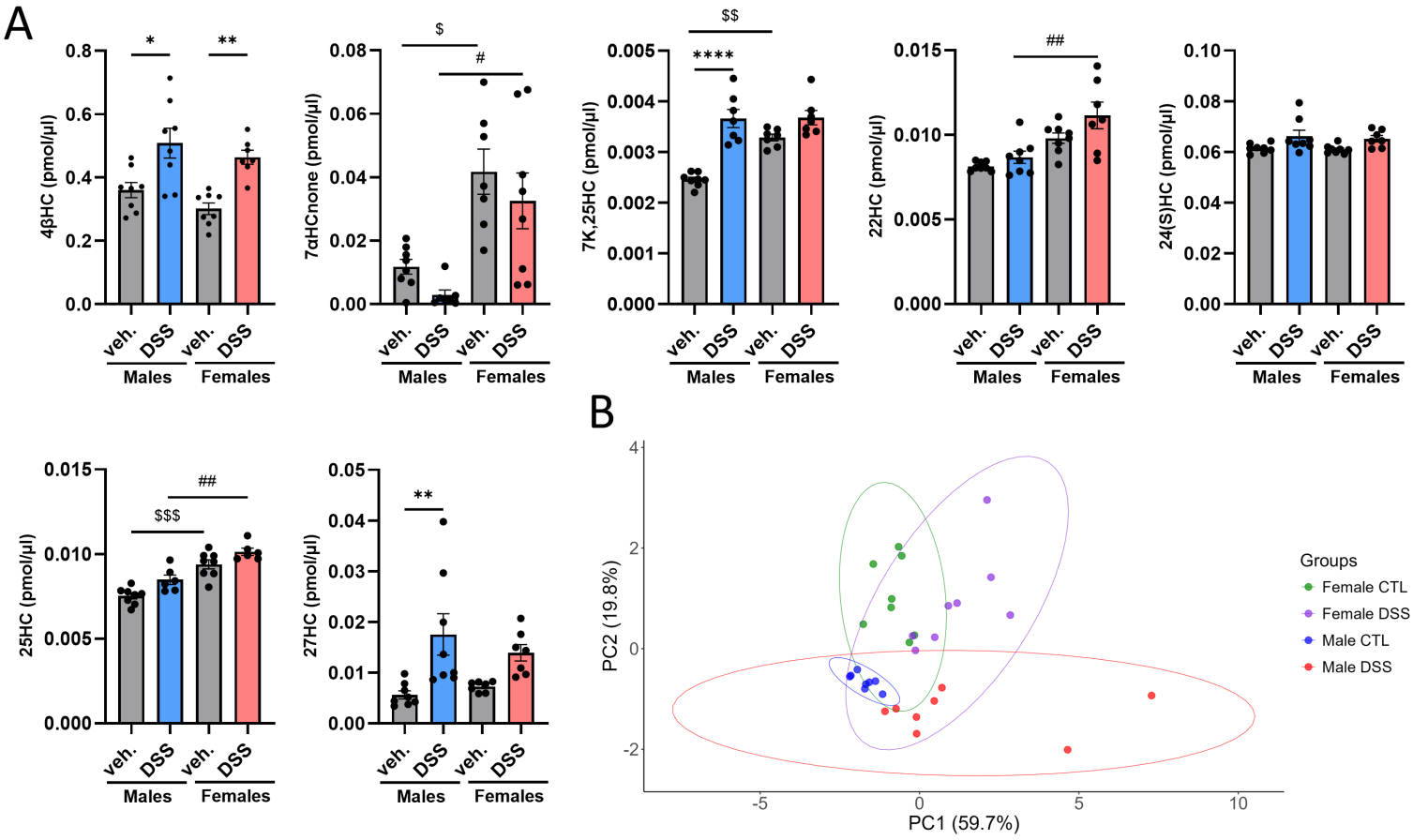
Male Mice Correlation Heatmap

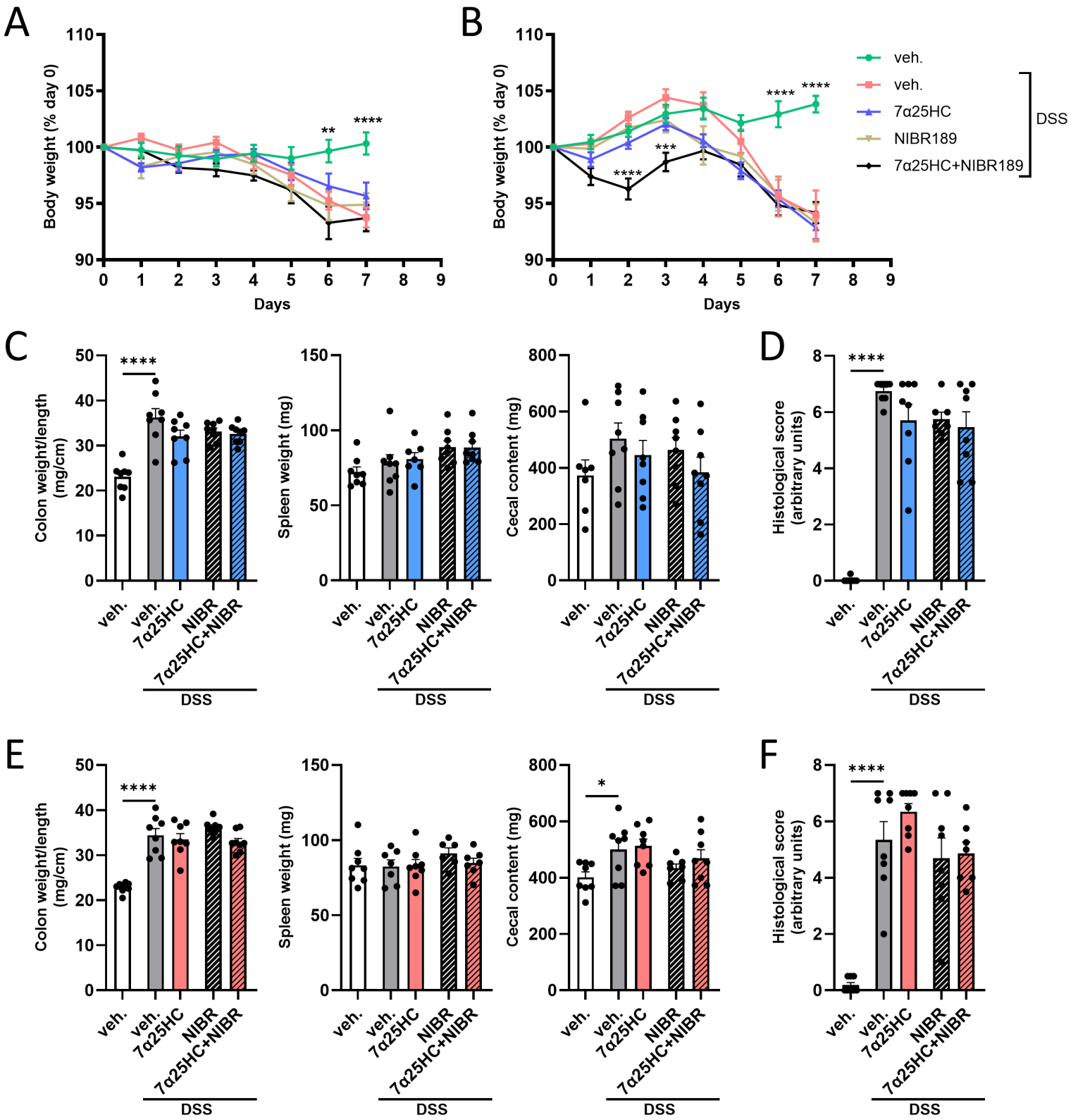
	TNF.α	MCP.1	IL.6	MPO	Colon.W.L
7K25HC	0.66**	0.75***	0.95***	0.50*	0.65**
24HC	0.34	0.35	0.66**	0.39	0.25
25HC	0.64**	0.55*	0.60*	0.38	0.50
27HC	0.47	0.58*	0.64*	0.70**	0.42
7αHCnone	0.17	-0.03	-0.20	-0.06	0.04
7HC	0.61*	0.65**	0.69**	0.45	0.54*
7KC	0.59*	0.56*	0.53*	0.31	0.43
5β.6β.epoxycholl	0.03	-0.04	-0.01	-0.18	-0.18
5α.6α.epoxycholl	-0.06	-0.15	-0.03	-0.35	-0.28
4βHC	0.74**	0.76***	0.73**	0.58*	0.71**

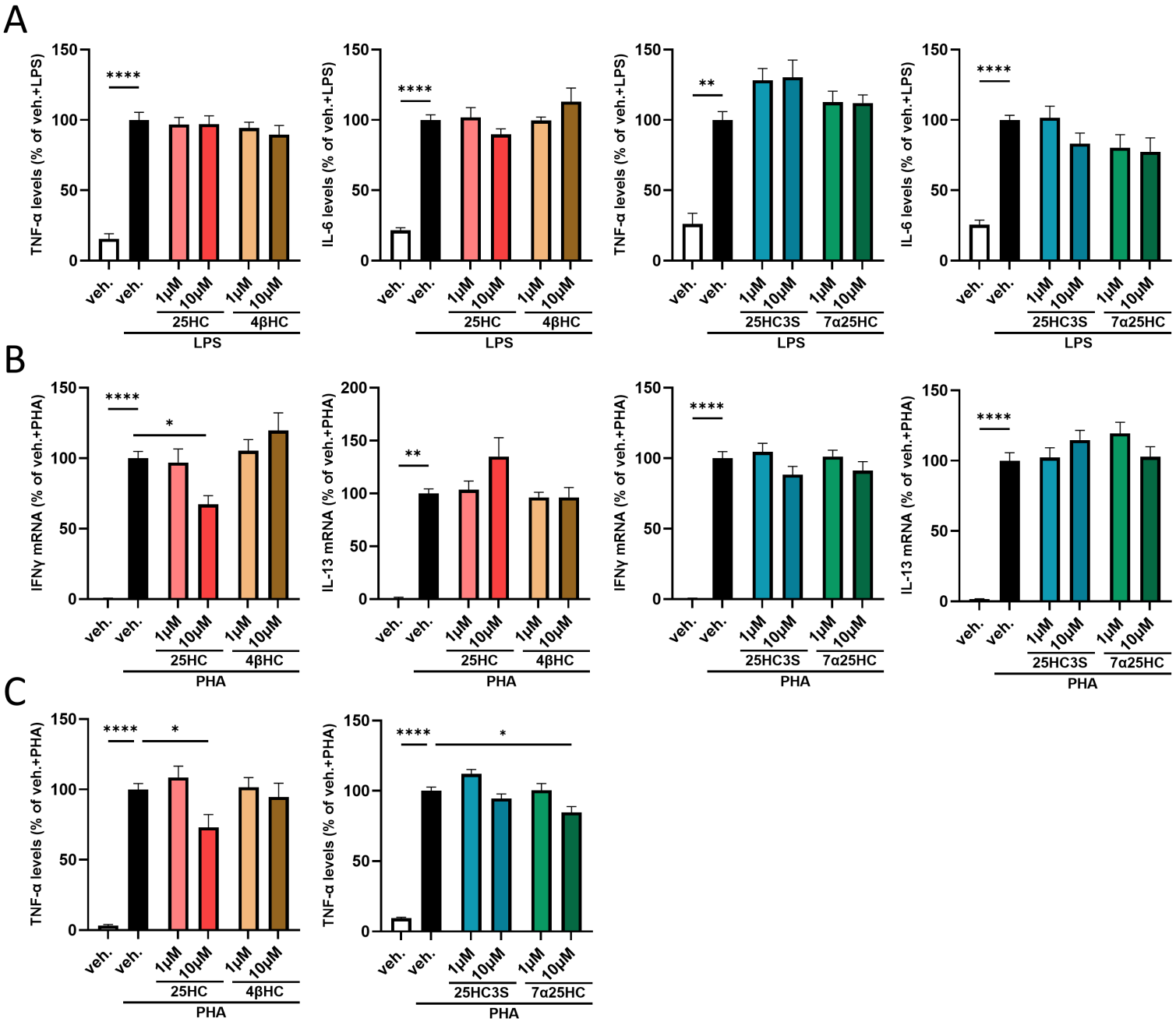
Female Mice Correlation Heatmap

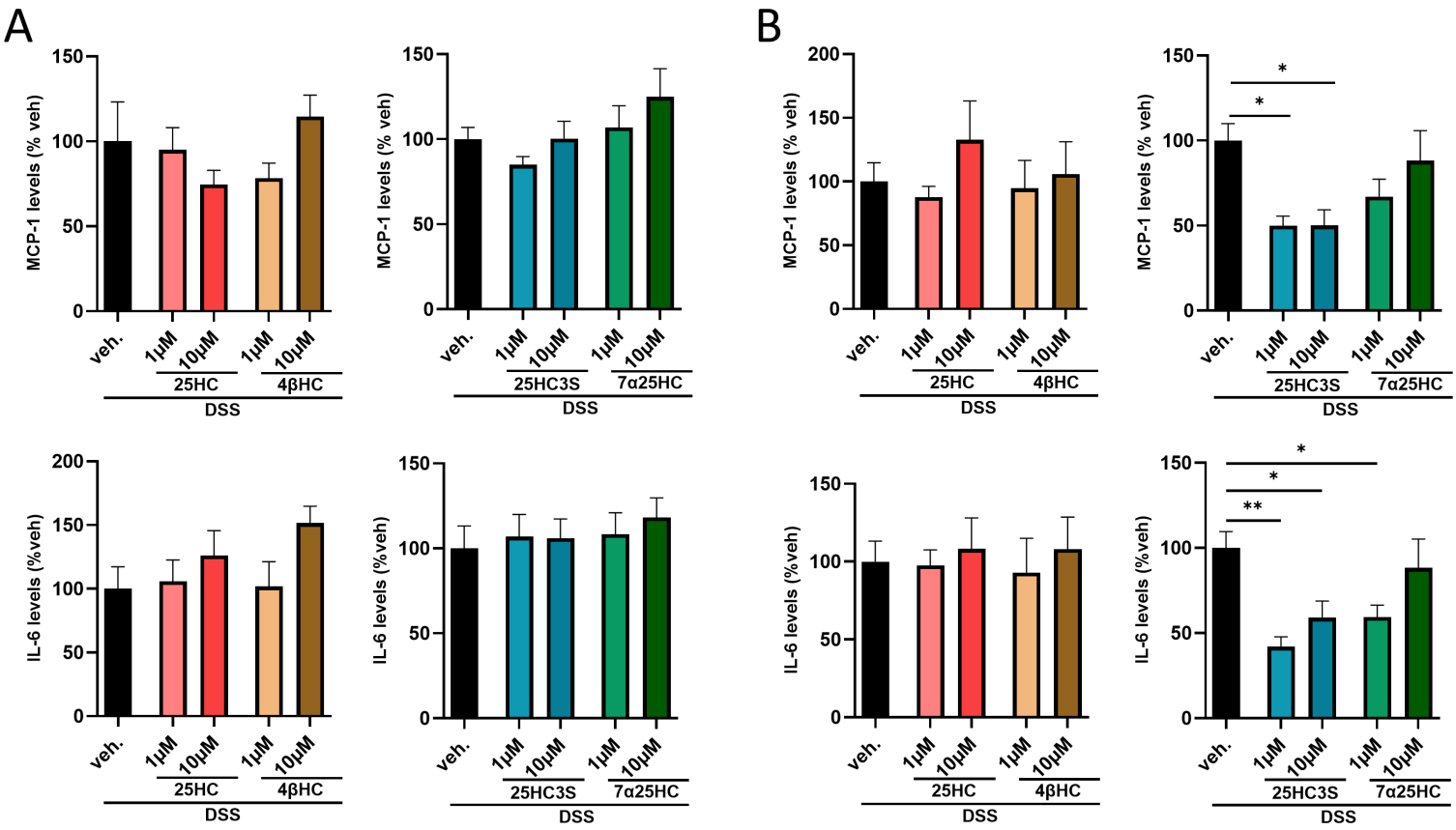
	TNF.α	MCP.1	IL.6	MPO	Colon.W.L
7K25HC	0.54*	0.44	0.28	0.67**	0.58*
24HC	-0.07	-0.04	-0.17	0.63**	0.37
25HC	-0.02	-0.27	-0.05	0.47	0.11
27HC	0.11	0.06	0.01	0.72**	0.54*
7αHCnone	0.07	-0.16	-0.27	0.69**	0.32
7HC	0.40	0.24	0.09	0.78***	0.52*
7KC	0.49	0.28	0.16	0.80***	0.61*
5β.6β.epoxycholl	0.05	-0.18	-0.23	0.58*	0.32
5α.6α.epoxycholl	-0.23	-0.24	-0.36	0.48	0.12
4βHC	0.17	0.03	-0.05	0.75***	0.41

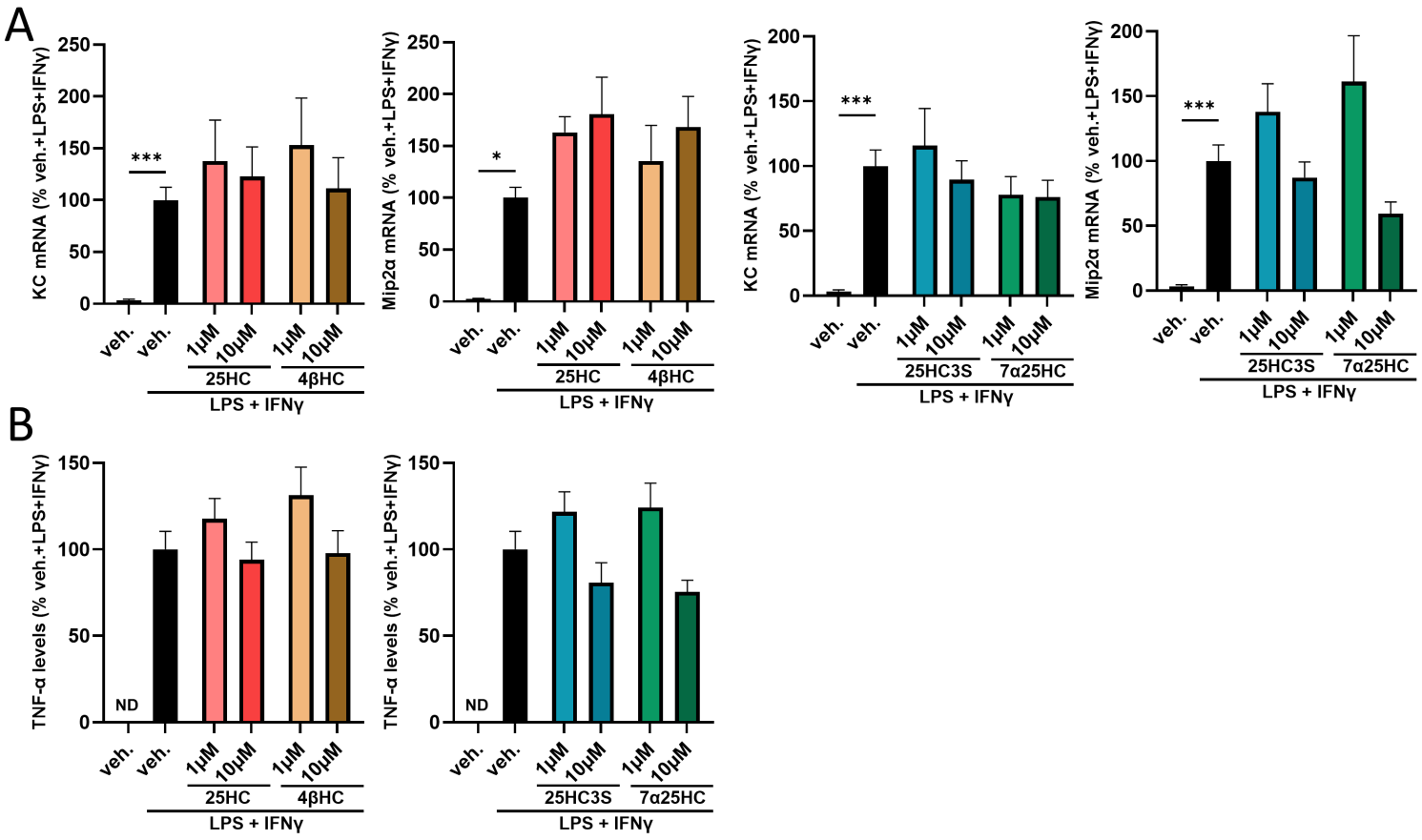
Correlation
1.0
0.5
0.0
-0.5
-1.0

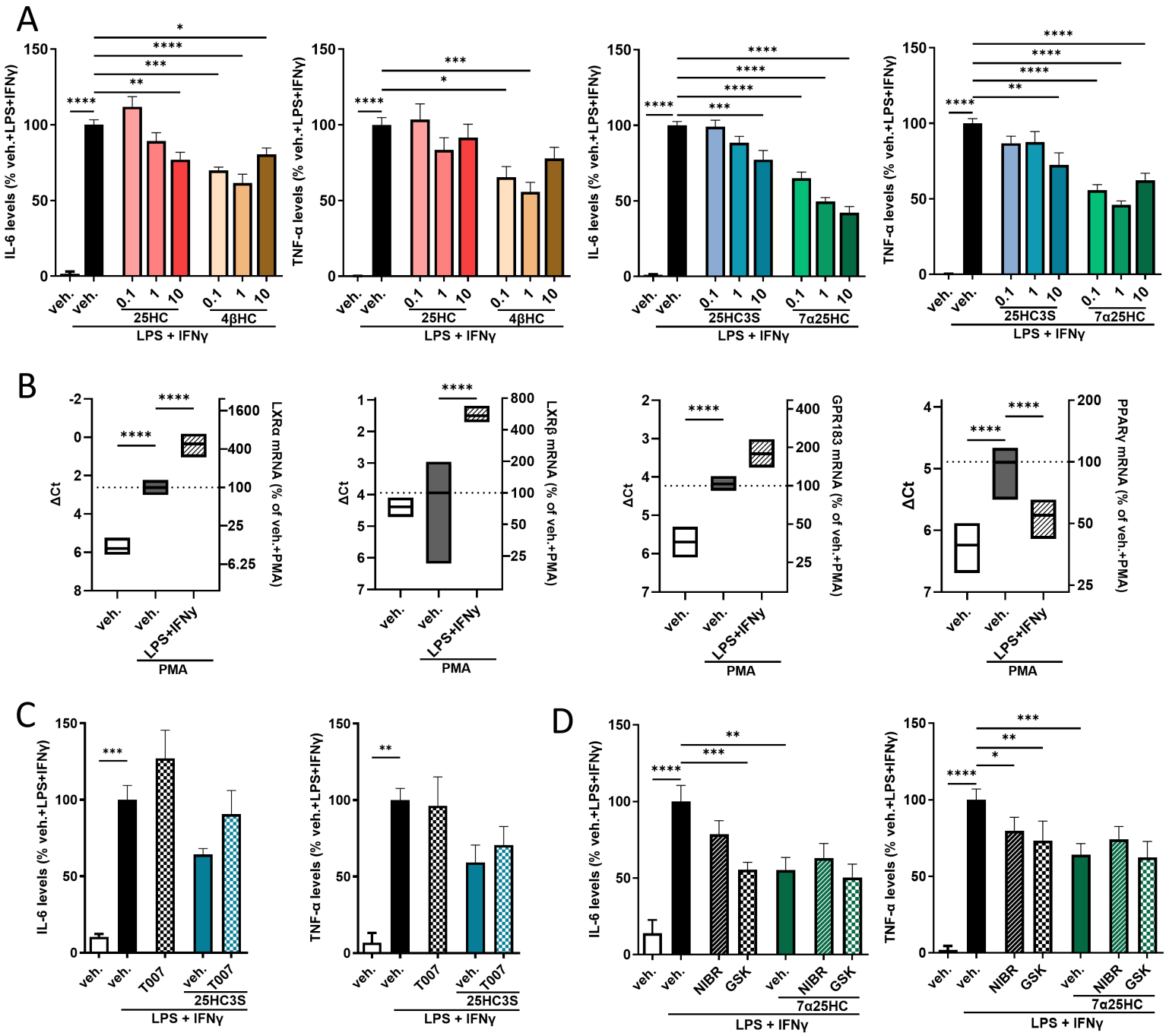

A
4βHC (pmol/µl)
7αHCnone (pmol/µl)
7K,25HC (pmol/µl)
22HC (pmol/µl)
24(S)HC (pmol/µl)
25HC (pmol/µl)
27HC (pmol/µl)
veh.
DSS
Males
Females
B
PC2 (19.8%)
PC1 (59.7%)
Groups
Female CTL
Female DSS
Male CTL
Male DSS


A
B
Body weight (% day 0)
Days
veh.
veh.
7α25HC
NIBR189
7α25HC+NIBR189
DSS
C
D
E
F
Colon weight/length (mg/cm)
Spleen weight (mg)
Cecal content (mg)
Histological score (arbitrary units)
veh.
veh.
7α25HC
NIBR
7α25HC+NIBR
DSS


A
TNF-α levels (% of veh.+LPS)
IL-6 levels (% of veh.+LPS)
TNF-α levels (% of veh.+LPS)
IL-6 levels (% of veh.+LPS)
****
****
**
****
veh.
veh.
1μM
10μM
25HC
4βHC
25HC3S
7α25HC
LPS
B
IFNγ mRNA (% of veh.+PHA)
IL-13 mRNA (% of veh.+PHA)
IFNγ mRNA (% of veh.+PHA)
IL-13 mRNA (% of veh.+PHA)
****
*
**
****
****
PHA
C
TNF-α levels (% of veh.+PHA)
TNF-α levels (% of veh.+PHA)
****
*
****
*
PHA


A
B
MCP-1 levels (% veh)
IL-6 levels (%veh)
150
100
50
0
200
veh.
1μM
10μM
25HC
4βHC
25HC3S
7α25HC
DSS
*
**


A
KC mRNA (% veh.+LPS+IFNγ)
Mip2α mRNA (% veh.+LPS+IFNγ)
KC mRNA (% veh.+LPS+IFNγ)
Mip2α mRNA (% veh.+LPS+IFNγ)
***
*
***
***
veh.
veh.
1μM
10μM
25HC
4βHC
25HC3S
7α25HC
LPS + IFNγ
B
TNF-α levels (% veh.+LPS+IFNγ)
TNF-α levels (% veh.+LPS+IFNγ)
ND
ND


A
IL-6 levels (% veh.+LPS+IFNγ)
TNF-α levels (% veh.+LPS+IFNγ)
veh.
0.1
1
10
25HC
4βHC
25HC3S
7α25HC
LPS + IFNγ
B
ΔCt
LXRα mRNA (% of veh.+PMA)
LXRβ mRNA (% of veh.+PMA)
GPR183 mRNA (% of veh.+PMA)
PPARγ mRNA (% of veh.+PMA)
LPS+IFNγ
PMA
C
T007
25HC3S
D
NIBR
GSK
7α25HC